Effect of High Pressure CO_2 Treatment on the Moisture Sorption Isotherm and Physicochemical Properties of Beef Jerky

by

Yanzhao Ren

A thesis submitted in partial fulfillment of the requirements for the degree of

Master of Science

in

Food Science and Technology

Department of Agricultural, Food and Nutritional Science
University of Alberta

Abstract

High pressure carbon dioxide (HPCD) treatment is a promising non-thermal pasteurization technique, targeting the enhancement of food safety by inactivating microorganisms without sacrificing quality. Even though this technique is effective for high moisture foods, research on products with a low water activity (a_w) is limited. Beef jerky, as a low a_w ready-to-eat snack, has become more popular because of the growing trend of high-protein and low-carb diets. The objective of this thesis research was to investigate the effects of HPCD treatment on the moisture sorption behavior and physicochemical properties of beef jerky.

Moisture sorption isotherms (MSIs), monolayer water content (M_0) and net isosteric heat of sorption (q_{st}) were determined under air and CO_2 environments at ambient pressure, as well as HPCD environment. MSI data were described mathematically by fitting into six isotherm equations. The deviation of the models used to fit the data increased under CO_2 atmosphere at ambient pressure and HPCD conditions. At ambient pressure, compared to the air environment, samples in CO_2 environment had higher a_w at a given moisture content. Under HPCD environment, the shape of MSIs changed from type II to type III and the isotherms became very steep at a_w levels of 0.73 and 0.70 at high pressures of 57 and 200 bar, respectively. Monolayer water content decreased with temperature, but pressure did not have a significant effect on M_0. Net isosteric heat of sorption in CO_2 environment was higher than that in air environment and the differential between the two environments decreased when the moisture content was increased.

The effects of HPCD processing parameters, including pressure, temperature, processing time and depressurization rate, on the physicochemical properties, including, a_w, surface color,

fat content, and Warner-Bratzler shear force, of beef jerky were studied by response surface methodology (RSM). Water activity decreased after HPCD treatment and temperature had a significant effect. In terms of surface color profile, *L*, *a, b* values increased after HPCD treatment and pressure had a significant effect on *L* value, no processing parameter showed a significant effect on *a* value, and pressure, quadratic pressure and depressurization rate had a significant effect on *b* value. After HPCD treatment, fat content of beef jerky was reduced slightly but no processing parameter had a significant effect. Warner-Bratzler shear force was either increased or decreased after HPCD treatment, where quadratic depressurization rate and linear temperature had a significant effect. An optimum HPCD treatment condition, that is, pressure of 92.9 bar, temperature of 59.1˚C*,* processing time of 35.9 min and depressurization rate of 56.3 bar/min, was determined via the RSM model to minimize the changes in responses.

The results obtained from this thesis research provide valuable information on further understanding of moisture sorption behavior during HPCD treatment that would contribute to elucidation of the microbial inactivation mechanism and the impact of HPCD treatment on the quality attributes of a low a_w food product like beef jerky.

Preface

This thesis is an original work by Yanzhao Ren under the supervision of Dr. Feral Temelli. There are a total five chapters in the thesis: Chapter 1 provides introduction and the overall objectives of this thesis study; Chapter 2 is a literature review on topics related to this research; Chapter 3 focuses on the effect of high pressure CO_2 environment on the moisture sorption isotherm of beef jerky; Chapter 4 investigates the effect of high pressure CO_2 treatment on the physicochemical properties of beef jerky; and Chapter 5 provides the overall conclusions and recommendations. These works were carried out by Yanzhao Ren by developing the specific experimental designs, experimental protocols, conducting experiments, performing data analysis and writing the first drafts and editing of the manuscripts under the guidance of Dr. Temelli. Of course, all of these works cannot be done without help from the people mentioned in the acknowledgements.

Manuscripts based on Chapters 3 and 4 are in preparation for submission to peer-reviewed journals for consideration for publication. Results of Chapter 3 were presented as a poster at the 17th European Meeting on Supercritical Fluids as "Effect of high pressure and CO_2 environment on the moisture sorption isotherm of beef jerky" by Yanzhao Ren and Feral Temelli in Ciudad Real, Spain on April 8-11, 2019.

Acknowledgements

I would especially like to thank my supervisor, Dr. Feral Temelli, for all of her guidance, help and support throughout all my research and graduate studies life. Without her advice, knowledge and encouragement, it is not possible for me to finish this research and thesis. She is not only the best guide in my research journey but also a great lifelong example for my personal development.

I would also like to thank my committee member, Dr. Lynn McMullen who provided significant advice to my research at committee meetings. Besides, she also supervised the preparation of the beef jerky sample. Also, I appreciate Dr. Heather Bruce being an examining committee member and to give me great advice and feedback for this thesis. Additionally, I thank Dr. Bruce for her support on the use of equipment to measure Warner-Bratzler shear force.

In addition, I thank Weijuan Huang and Dr. Lingyun Chen for the use of equipment and technical support on the Warner-Bratzler shear force measurement.

I am grateful for the funding sponsored by Alberta Innovates and Alberta Agriculture and Forestry for the project entitled "An innovative CO_2-decontamination technology to ensure food safety of low water activity food products". My MSc research was part of this larger project.

Lastly, I would like to express my appreciation to all my friends and family as well as lab mates in 2-51 who contributed their time and effort in helping with my project and life.

Table of Contents

List of Tables

List of Figures

List of Abbreviations

a	Hunter color index a, red-green
A, B, C	Constants
ANOVA	Analysis of variance
a_w	Water activity
AWM	a_w measurement
b	Hunter color index b, blue-yellow
CCRD	Central composite rotatable design
CO_2	Carbon dioxide
d	Desirability
DR	Depressurization rate
E	Mean relative percentage deviation
HH	Hailwood and Horrobin equation
H-IC	Halsey-Iglesias and Chirife equation
HPCD	High pressure carbon dioxide
IC	Iglesias and Chrife equation
GAB	Guggenheim, Anderson and de Boer equation
k	Number of independent parameters
L	Hunter color index L, lightness
M_0	Monolayer water content
M, MC	Moisture content
MSI	Moisture sorption isotherm
N	Newtons
P	Pressure
P_c	Critical pressure
q_{st}	Heat of sorption
R	Gas constant R=8.314 J/(mol-K)
RSM	Response surface methodology
SDS-PAGE	Sodium dodecyl sulfate-polyacrylamide gel electrophoresis

SSS	Saturated salt slurry
t	Processing time
T	Temperature
T_c	Critical temperature
WBSF	Warner-Bratzler shear force
$\bar{V}_L$	Molar volume of the liquid
x_{H2O}	Mole fraction of H_2O
$X_i\ X_j$	Coded process variables
Y	Responses of untreated sample
Y'	Responses of treated sample
$\Delta\ Y$	Response differences
β_0	Constant
β_i	The first degree coded input parameters
β_{ii}	The second degree coded input parameters
β_{ij}	The interaction of linear parameters
$\in$	Error term

Chapter 1: Introduction and objectives

Generally, low water activity (a_w) foods (a_w<0.85) are considered as shelf-stable at ambient temperature because low a_w places osmotic stress on bacteria and less water is available for bacterial growth (Borowski, Ingham, and Ingham, 2009; Kimber, Kaur, Wang, Danyluk, and Harris, 2012; FAO. WHO, 2015). Normally, low a_w foods like nuts may have a year or more of shelf life. However, numerous studies have demonstrated that *Escherichia coli* and *Salmonella* can survive on low a_w foods (Hiramatsu, Matsumoto, Sakae and Miyazaki, 2005; Gruzdew, Pinto and Sela Saldinger, 2012). These microorganisms can grow and cause infections upon reaching the gastrointestinal tract after ingestion of a contaminated product and seriously threaten the health of consumers (Aviles, Klotz, Smith, Williams and Ponder, 2013).

CO_2 has been used as an antimicrobial agent for more than 100 years because of its natural characteristics, including microbial inhibition effect near atmospheric pressure, being non-toxic and that it can be easily removed from food products (Valley and Rettger, 1927; Jones and Greenfield, 1982; Eklund, 1984; Dixon and Kell, 1989). More recently, it has been found that pressurised CO_2 is no longer bacteriostatic, but bactericidal (Nakamura et al., 1994; Enomoto et al., 1997; Erkmen, 2000; Calvo and Balcones, 2001; Garcia-Gonzalez et al. 2007). High pressure CO_2 (HPCD) treatment as a food processing technique was found to show a microbial inactivation effect. However, microbial inactivation strongly depends on a_w of the food where low a_w products are more challenging to treat. Haas et al. (1989) even suggested that a HPCD treatment would not be applicable to dry substances. On the contrary, Dillow, Dehghani, Hrkach, Foster and Langer (1999) reported that *E. coli* cells were inactivated by HPCD in the absence of water.

According to Statistica (2019), there is a growing demand for beef jerky due to its convenience, nutritional value as a protein source, and the popularity of low-carb and low-fat diets. Schultze (2019) found that *E. coli* AW 1.7, MG1655 and the Shiga toxin-producing *E. coli* cocktail inoculated onto beef jerky were inactivated successfully by treatment with CO_2 saturated with water at 65 ˚C and 57 bar for 15 min. Therefore, for beef jerky, HPCD is a promising non-thermal pasteurisation technology to extend its shelf life and enhance its safety with a minimal change in its nutritional value. However, some studies reported that HPCD treatment can lead to a change in physicochemical properties, including surface colour and tenderness of meat products (Cappelletti, Ferrentino and Spilimbergo, 2015). Nevertheless, available literature focusing on the effects of HPCD treatment on the physicochemical quality of meat products is limited to provide guidance in this regard.

Moisture plays an important role in microbial inactivation by HPCD and HPCD treatment can have an impact on the physicochemical properties of a food product. However, the literature lacks information on these aspects. Therefore, it was hypothesized that:

1) HPCD environment affects the moisture sorption behavior of beef jerky; and

2) HPCD treatment affects the physicochemical properties of beef jerky.

The objectives of this thesis research were to:

1) study the moisture sorption behavior of beef jerky under HPCD conditions (Chapter 3); and

2) investigate the influence of HPCD treatment parameters on the physicochemical properties of beef jerky (Chapter 4).

Chapter 2: Literature review

2.1 High pressure carbon dioxide (HPCD) treatment and microbial inactivation

2.1.1 HPCD treatment

High pressure CO_2 (HPCD) technique refers to treating foods with either sub- or supercritical CO_2 for a certain period of time in a batch, semi-continuous or continuous manner. Supercritical CO_2 is CO_2 at a temperature and pressure above its critical point (T_c=31.1 ˚C, P_c=73.8 bar), and exhibits the unique ability to diffuse through solids like a gas, and dissolve different solutes like a liquid. Subcritical CO_2 is CO_2 at a temperature or pressure below its critical point values (Garcia-Gonzalez et al., 2007). HPCD has antimicrobial effects in various liquid and solid food systems (Garcia-Gonzalez et al., 2007). For example, Wei, Balaban, Fernando and Peplow (1991) found that HPCD could reduce *Listeria* in shrimp, orange juice and egg yolk and *Salmonella* in chicken and egg yolk effectively. As a solvent, CO_2 is relatively inert, inexpensive, non-toxic, non-flammable, recyclable, readily available in high purity, and leaves no residue (Choi et al., 2007). Additionally, HPCD technique is classified as a cold pasteurization method because application of relatively low temperatures can result in inhibition of microorganisms. Compared to heat treatment, HPCD is believed to involve fewer changes in taste, color, texture and nutritional quality in foods (Damar and Balaban, 2006). As a result, HPCD can be applied as a processing aid to foods. According to Health Canada, a processing aid is defined as “a substance that is used for a technical effect during food processing or manufacture but, unlike food additives, its use does not affect the intrinsic characteristics of the food and it results in no or negligible residues of the substance or its by-products in or on the finished food” (Health Canada, 2018). Therefore, HPCD is a promising clean-label technology to

extend food shelf life with minimal changes in quality because processing aids do not need to be disclosed on labels (Health Canada, 2018).

2.1.2 Mechanism of microbial inactivation

As an alternative non-thermal pasteurization technique for foods, the pressures employed during HPCD treatment, compared to high hydrostatic pressure (HHP) technique, are much lower (generally <200 bar) than that used in HHP (~3000-6000 bar). However, the exact inactivation mechanisms still remain to be unraveled. Garcia-Gonzalez et al. (2007) summarized comprehensively how HPCD exerts its lethal action on bacteria in the following steps. Garcia-Gonzalez et al. (2007) emphasized that these steps will not occur consecutively but rather take place simultaneously in a complex and interrelated manner.

2.1.2.1 Solubilization of CO_2 in the external liquid phase

In foods with a high water content, CO_2 can dissolve in the water to form carbonic acid, which dissociates into bicarbonate (HCO_3^-), carbonate (CO_3^{2-}) and hydrogen (H^+) ion species according to the following equilibria (Eq. 2.1-2.4) (Garcia-Gonzalez et al., 2007):

$CO_2\,(g) \leftrightarrows CO_2\,(aq)$

$[CO_2]_{aq} = H * p_{CO2}$ with $H = 3.3*10^{-2}$ mol/ (L atm) (25 ˚C) (2.1)

$CO_2\,(aq) + H_2O \leftrightarrows H_2CO_3$

$[H_2CO_3]/\,[CO_2]_{aq} = 1.7 * 10^{-3}$mol/L (25 ˚C) (2.2)

$H_2CO_3 \leftrightarrows H^+ + HCO_3^-$

$[HCO_3^-]\,[H^+]/[H_2CO_3] = 2.5 * 10^{-4}$ mol/L (25 ˚C) (2.3)

$HCO_3^- \boxed{\leftrightarrow} H^+ + CO_3^{2-}$

$[CO_3^{2-}] [H^+]/[HCO_3^-] = 5.61 * 10^{-11}$ mol/L (25 ˚C) (2.4)

As a consequence, external water in contact with HPCD becomes acidic due to the formation and dissociation of H_2CO_3. The decrease in external pH may inhibit microbial growth (Hutkins and Nannen, 1993) and increase energy consumption by bacteria to maintain homeostasis (Hong, Park and Pyun, 1999). However, the reduction of external pH cannot fully explain the inactivation effect of HPCD because stronger acids like hydrochloric acid or phosphoric acid cannot exert a comparable reduction (Haas et al., 1989; Wei, Balaban, Fernando, and Peplow, 1991; Lin et al., 1993; Debs-Louka, Louka, Abraham, Chabot and Allaf, 1999).

2.1.2.2 Cell membrane modification

Because of the high affinity between CO_2 and the plasma membrane, CO_2 can be dissolved in the phospholipids of a model cell membrane to a high extent (Spilimbergo, 2002). Jones and Greenfield (1982) also suggested that the HCO_3^- ion may act on the charged phospholipid head groups and the proteins on the membrane. Due to the presence of dissolved CO_2 and HCO_3^-, the cell membrane can be modified structurally and functionally (Jones and Greenfield, 1982; Isenschmid, Marison and Von Stockar, 1995).

2.1.2.3 Intracellular pH decrease

With CO_2 penetrating through the bacterial cell membrane, more CO_2 accumulates in the cytoplasm of the cells. Inside the cell, CO_2 acts as a reactant and shifts the equilibrium to the products, resulting in the formation of carbonic acid and carbonate, bicarbonate and hydrogen ions (Eq. 2.1-2.4). At the beginning, the cell attempts to maintain homeostasis using pH

buffering systems, including cytoplasmic buffering, proton pumps, membrane-bound H^+-ATPases, and the production of acids or bases (Booth, 1985; Hutkins and Nannen, 1993). However, the intracellular pH would start decreasing after the buffering ability is exceeded (Damar and Balaban, 2006; Garcia-Gonzalez et al., 2007). According to Spilimbergo, Bertucco, Basso and Bertoloni (2005), intracellular pH of *Bacillus subtilis* decreased to 3.3 upon HPCD exposure (8 MPa, 30 ˚C, 5 min).

2.1.2.4 Key enzyme inactivation/cellular metabolism inhibition

According to Hutkins and Nanen (1993), the lowering of the cytosolic pH might significantly impact the activity of key enzymes, involved in essential metabolic and regulating processes for the bacteria cell, such as glycolysis, amino acid and peptide transport, active transport of ions and proton translocation. According to Hong and Pyun (2001), some enzymes lost their activities significantly by HPCD treatment in *Lactobacillus plantarum*. Spilimbergo (2002) also found that several enzymes were inactivated by HPCD treatment in *B. subtilis*.

In addition to pH, the concentrations of CO_2 and HCO_3^- are also important in the regulation of enzymatic activity by either promoting or inhibiting carboxylation and decarboxylation reactions (Jones and Greenfield, 1982). Specifically, CO_2 is a substrate in the carboxylation reaction and a product in the decarboxylation reaction. As a result, cell metabolism is affected with increasing concentration of CO_2 by regulating equilibrium balance of these metabolic reactions (Jones and Greenfield, 1982).

2.1.2.5 Disordering of the intracellular electrolyte balance

According to Lin et al. (1993), intracellular inorganic electrolytes, including Ca^{2+} and Mg^{2+} could precipitate in the presence of CO_3^{2-}. These inorganic electrolytes play important roles

not only in a large number of cell activities but also in maintaining the osmotic relationships between cells and their surrounding media. Additionally, collapse of the proton motive force across the membrane disorders cytosolic Ca^{2+} levels, because Ca^{2+} extrusion is catalyzed by a Ca^{2+}/H^{+} antiporter driven by the proton motive force (Gangola and Rosen, 1987).

2.1.2.6 Removal of vital constituents

Last but not least, the physical disruption of cells was the first explanation for the bacterial inactivation after release of CO_2. HPCD treatment involving rapid depressurization results in the expansion of CO_2 in the cells, leading to cellular disruption (Damar and Balaban, 2006). Besides, Kmihira, Taniguchi and Kobayashi (1987) and Lin et al. (1992, 1993) reported that CO_2 could extract vital constituents from the cell or cell membranes because of its relatively high solvating power, especially under supercritical conditions. The removal of constituents not only disturbs the structure of the bio-membrane but also alters the balance of the biological system, and as a result, promoting inactivation (Lin et al., 1992, 1993).

2.1.3 Importance of water

2.1.3.1 Effect of moisture content

Different studies have shown that foods with a low moisture content were poorly inactivated by HPCD (Haas, Prescott, Dudley, Dik, Hintlian, and Keane, 1989; Nakamura, Enomoto, Fukushima, Nagai and Hakoda, 1994; Kumagai, Hata and Nakamura, 1997; Debs-Louka, Louka, Abraham, Chabot and Allaf, 1999; Schmidt, Beermann, Bach and Schollmeyer, 2005). For example, Kumugai et al. (1997) found the first order sterilization rate constant to be almost zero at a moisture content below 0.2 g/g of dry matter, and the sterilization rate tended to increase with increasing moisture content of up to 1 g/g of dry matter. The reason

for why dry microbial cells are more challenging to be inactivated by HPCD is probably the result of a decrease in the amount of CO_2 solubilized in the dry cell (Steps 1 and 3 in mechanism of inactivation). The acidification of the extra- and intra-cellular environment through dissociation reaction is dependent on the presence of water. An increased amount of formation and dissociation of H_2CO_3 would release more H^+ ions that reduce the pH of the external suspending medium (Step 1 of the mechanism of inactivation). Additionally, Lin, Yang and Chen (1993) attributed the synergistic effect of water to swollen cell walls and membranes so that these biological barriers become more penetrable by CO_2.

2.1.3.2 Water-CO_2 interactions

To better understand the impact of HPCD treatment on low a_w products, it is also necessary to understand how water behaves under HPCD environment. The solubility of water in HPCD was studied by different researchers (Chrastil, 1982; King, Mubarak, Kim and Bott, 1992; Bamberger, Sieder, and Maurer, 2004; Tabasinejad et al., 2011; Ahmad, Gersen, and Wilbers, 2014; Comak et al., 2016). Recently, Wang, Zhou, Guo, Yang, and Lu (2018) determined the water solubility in supercritical CO_2 from 40 to 200 ˚C and from 100 to 500 bar by in-situ quantitative Raman spectroscopy (Fig. 2.1). Wang et al. (2018) found that at constant pressure, water solubility in HPCD increases exponentially with increasing temperature. At low temperatures (40-100 ˚C), water solubility increases with increasing pressure, but at high temperatures (140-200 ˚C), water solubility decreases with increasing pressure. From 100 to 140 ˚C, water solubility first decreases with increasing pressure (pressure < 20 bar), and then increases with increasing pressure (pressure > 20 bar).

The intermolecular interaction of water in HPCD as a solvent was studied by some authors (Tucker, 1999; Kajimoto, 1999) but they reached different conclusions. Clarke, Harrison,

Johnston, and Howdle (1997) concluded that water is almost free in HPCD (T=32 ˚C, P=156 bar) environment. In contrast, Bowman et al. (1996) argued that the rotation of water in CO_2 was hindered because of dipole-quadrupole interaction between water and CO_2. Tassaing, Oparin, Danten, and Besnard (2005) studied water-CO_2 interaction in supercritical CO_2 by infrared spectroscopy and vibrational frequency shift calculation. Tassaing et al. (2005) found that dispersive and dipole-quadrupole interactions are dominant in the stabilisation energy of water-CO_2 pair, and that water acts as an attractive solute (the attractive forces between water and CO_2 leading to the clustering of solvent molecules around water) in the hyper-compressible regime in the vicinity of the critical point of the solvent.

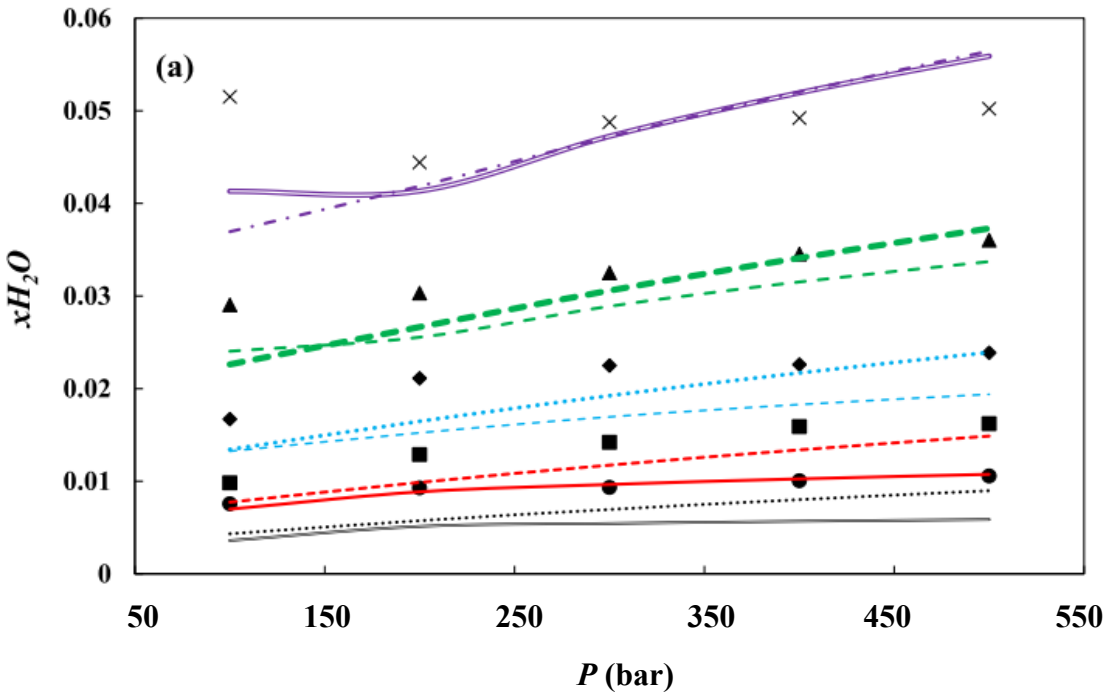

Figure 2.1. Water solubility in CO_2 (x_{H2O}) as a function of pressure (P). ●, 40 ˚C; ■, 60 ˚C; ◆, 80 ˚C; ▲, 100 ˚C; ×, 120 ˚C, Predictions from Duan, Hu, and Sun (2003): ——, 40 ˚C; ——, 60 ˚C; ------, 80 ˚C; ------, 100 ˚C; ═══, 120 ˚C. Prediction from Aavatsmark and Kaufmann (2015): ·····, 40 ˚C; ------, 60 ˚C; ·····, 80 ˚C; ▬ ▬, 100 ˚C; –·–, 120 ˚C. Reprinted from Wang et al. (2018) with permission from Elsevier.

According to Ferrentino, Calix, Poletto, Ferrari and Balaban (2012), CO_2 solubility in water also increases with pressure and temperature. As a result of CO_2 solubilization in H_2O, the volume of liquid water phase was found to increase (Fig. 2.2) in HPCD environment and the relative volumetric expansion of water increased up to 14.4%, 12.3% and 10.2% at 40, 50 and 60 ˚C, respectively, at 300 bar (Zhao, Temelli, Curtis and Chen, 2015).

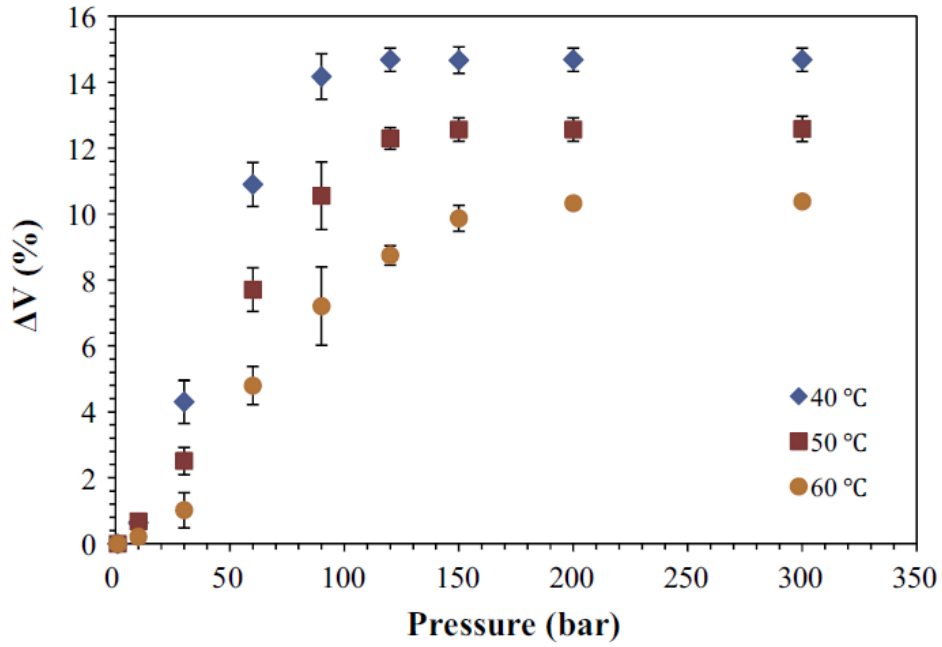

Figure 2.2. Relative volumetric expansion of water in equilibrium with CO_2 as a function of pressure at different temperatures. Reprinted from Zhao, Temelli, Curtis and Chen (2018) with permission from Elsevier.

2.2 Moisture sorption isotherm (MSI)

2.2.1 Water in a food matrix and classification of MSI

In biological systems such as foods, water exists with unhindered or hindered mobility and is colloquially referred to as free water and bound water, respectively (Fig. 2.3). Free water behaves similar to liquid water, whereas bound water is defined as sorbent- or solute-associated

water that differs thermodynamically from pure water (Berlin, 1978). The bound water is reported to be bound to stronger hydrogen bond acceptors than liquid water as well as water-solvating nonpolar groups. Bound water has a reduced solubility for other compounds, and it is not freezable, not available for chemical reactions or for microbial growth or as plasticizer, and it shows a decrease in its diffusion coefficient with decreasing moisture content (Luck, 1981; Al-Muhtaseb et al., 2002; Rao et al., 2014).

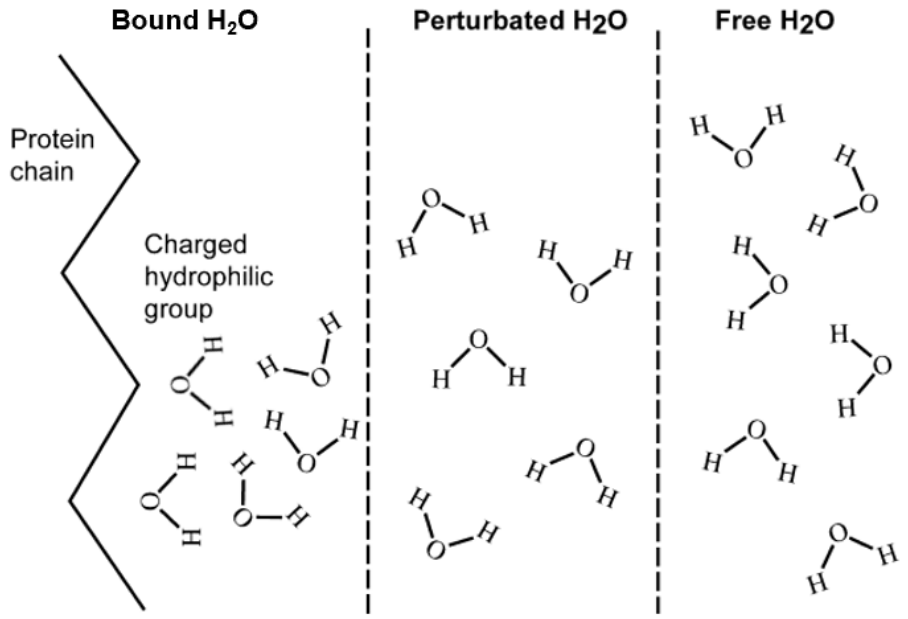

Figure 2.3. Strongly associated, perturbated, and "free" water in a food matrix. Reprinted from Labuza and Albunakar (2007) with permission from Wiley Books.

To investigate the reasons behind why low a_w food products are poorly inactivated by HPCD, it is essential to understand the role water plays in food. Moisture sorption isotherm (MSI) is a useful tool to understand the thermodynamic properties involved in the sorption behavior of water in foods; however, such information is missing for foods placed in a HPCD environment. The knowledge of thermodynamic properties can provide insights into the microstructure

associated with a food, as well as theoretical interpretations of the physical phenomena occurring at food-water interfaces (Rao, Rizvi, Datta and Ahmed, 2014).

MSI represents the relationship between total moisture content (MC) and the corresponding a_w of a food over a range of values at a constant temperature and pressure. The a_w of food is defined as the ratio of the water vapor pressure in food (P_w) to the vapor pressure exerted by pure water (P°_w) at the same temperature, as shown in Eq. (2.5)

$$a_w = P_w/P^\circ_w \tag{2.5}$$

Adsorption isotherms are generated by placing a dry material into atmospheres of high relative humidity and measuring the weight gain due to water uptake, which can be considered as physical adsorption referring to the adherence of molecules of a gas on a surface at a lower pressure than the pressure of steam (Nieto, 2010). The isotherms, product of the physical adsorption, can be grouped into five types (Fig. 2.4) according to Brunauer, Deming, Deming and Teller (1940). Types II and III are closely related to types IV and V, except that the maximum adsorption occurs at some pressure lower than the vapor pressure of the gas. In other words, types IV and V suggest that the complete or almost complete filling of the pores and capillaries of the adsorbent occurs at a pressure lower than the vapor pressure of the gas, sometimes at a considerably lower pressure. Interpretation of the different types of isotherms is shown in Table 2.1.

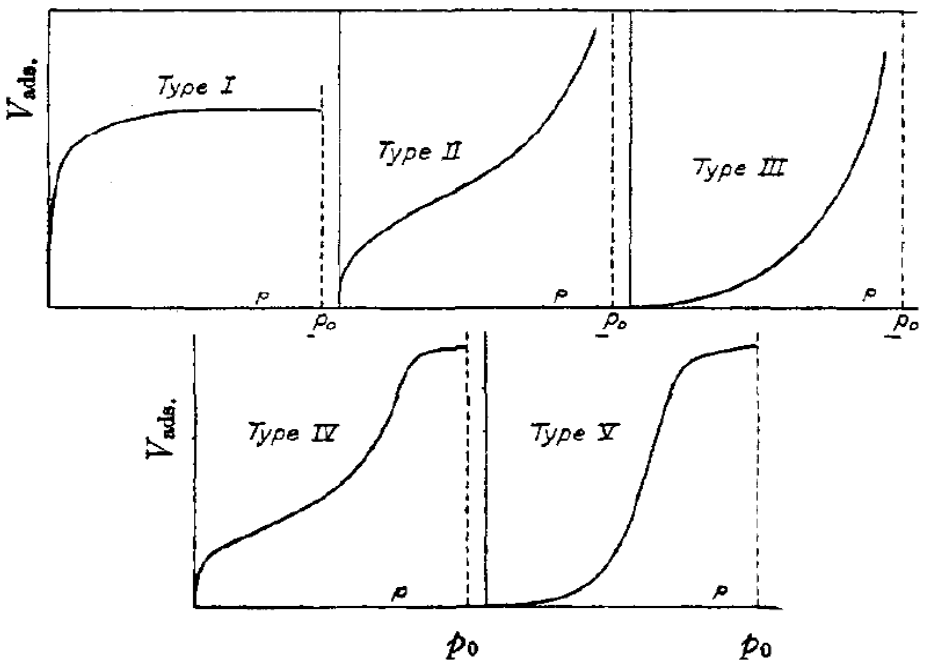

Figure 2.4. Five types of moisture sorption isotherms. Reprinted from Brunauer et al. (1940) with permission from American Chemical Society.

Table 2.1. Classification of physical adsorption isotherms. Reprinted from Condon (2006) with permission from Elsevier.

Type	Type interpretation
I	This is characteristic of either a chemisorption isotherm (in which case the final upswing at high pressure may not be present) or physisorption on a material that has extremely fine pores (micropores).
II	This is characteristic of a material, which is not porous, or possibly microporous, and has a high energy of adsorption.
III	This is characteristic of a material, which is not porous, or possibly microporous, and has a low energy of adsorption.
IV	This is characteristic of a material, which contains mesoporosity and has a high energy of adsorption. These often contain hysteresis attributed to the mesoporosity.
V	This is characteristic of a material, which contains mesoporosity and has a low energy of adsorption. These often contain hysteresis attributed to the mesoporosity.

MSIs of most foods are nonlinear, generally sigmoidal in shape, and have been classified as type II isotherm. According to Labuza and Albunakar (2007), the sigmoidal shape is caused by the additive effects of Raoult's law, capillary effect and surface-water interactions. In a typical type II isotherm, there are two bending regions, one around an a_w of 0.2-0.4 and another at 0.6-0.7. According to Al-Muhtaseb, McMinn and Magee (2002), most of the water in fresh foods exert a vapor pressure very close to that of pure water and this vapor pressure level is maintained until the moisture content of food decreases to about 22%. Then, the moisture level is no longer able to sustain the vapor pressure of food at unity, and therefore, begins to show a lowered vapor pressure. The changes with atmosphere humidity of this last fraction of water in dehydrated foods result in the characteristic sigmoidal shape of MSI.

Foods rich in soluble components, such as sugar or salt, display type III behavior (Rao, Rizvi, Datta and Ahmed, 2014). However, if the solid is porous so that it has an internal surface, then the thickness of the adsorbed layer on the wall of the pores is necessarily limited by the width of the pores and the form of the isotherm is modified accordingly (Table 2.1).

2.2.2 Measurement of MSI

Commonly, MSI is determined by the saturated salt slurry (SSS) method, where the food material is placed over saturated salt slurries with specific a_w values in closed chambers and stored until the food reaches the same a_w as the saturated salt slurry. However, this method has disadvantages in terms of requiring cumbersome labor, microbial deterioration of sample at a_w>0.6 and the need for a long time (normally from weeks to months) to reach equilibrium.

An alternative approach is the a_w measurement (AWM) method, which can be used to generate the MSIs in a relatively short period of time. AWM method was proposed by Bell and

Labuza (2000) and the basic principle is measuring the water activity of a sample when the water content is fixed. Specifically, a real test by AWM requires the following steps for generating an adsorption isotherm (Zhang, Sun and Zhang, 2017):

1. Moisture adjustment: change the amount of water in the target samples to several levels by mild dehydration;
2. Moisture adsorption: wet the sample by spraying water directly or by exposing to humid atmosphere;
3. Moisture redistribution: samples with various water contents need to be sealed separately and stored for a period time for complete moisture redistribution in samples; and
4. Measurement of a_w and water content: a_w and water content are measured and thus one data point is generated.

Compared with the SSS method, AWM method expedites the experimental process to as low as tens of minutes and hours (Demarchi et al., 2013; Argyropoulos and Muller, 2014). In addition, a large number of data points can be generated by simply adjusting the rewetting time.

2.2.3 Effects of processing parameters on MSI

Because the a_w is an equilibrium concept, any single or combined processing effect might change the adsorbing sites. In this section, the effects of temperature, pressure, and combined temperature-pressure on moisture sorption isotherms are discussed (Labuza and Albunakar, 2007).

2.2.3.1 Temperature effect on MSI

During measuring and describing the MSI, the temperature has to be specified and held constant because temperature affects the mobility of water molecules and the dynamic equilibrium between the vapor and adsorbed phases (Labuza, 1971; Kapsalis, 1981). In general, temperature has an increasing effect on a_w at constant moisture content and this effect is greatest at lower to intermediate water activities (Fig. 2.5). This is because of the nature of water binding; at constant a_w, foods that follow the type II isotherm hold less water at higher temperatures than at lower temperatures (Labuza and Albunakar, 2007). Additionally, at high a_w and temperature, some new solutes may dissolve causing a crossover of isotherms at high a_w (Fig. 2.5). Above an a_w value of 0.8, no temperature effect was observed.

Labuza (1968), Loncin (1980), and Iglesias and Chirife (1976a) have shown that the Clausius-Clapeyron equation can be applied to predict the a_w value at any temperature if the corresponding excess heat of sorption is known at constant moisture content. The effect of temperature follows the Clausius-Clapeyron equation (Eq. (2.6)):

$$\ln\frac{a_{w2}}{a_{w1}} = \frac{q_{st}}{R}\left(\frac{1}{T_1} - \frac{1}{T_2}\right) \tag{2.6}$$

where a_{w2} and a_{w1} are the a_w at temperatures T_2 and T_1, respectively; q_{st} is the heat of sorption in J/mol (as a function of moisture content), and R equals 8.314 J/(mol K).

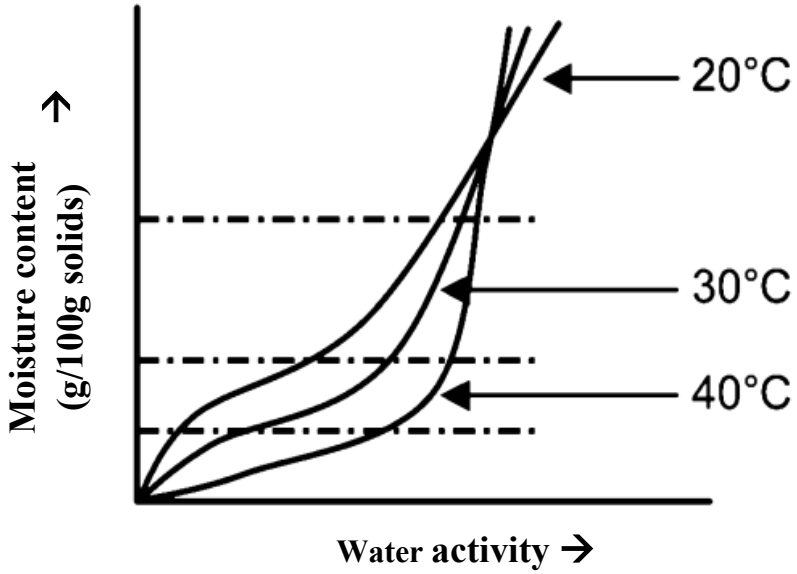

Figure 2.5. Water activity change for a food subjected to a temperature shift (Labuza, 1984). Reprinted from Labuza and Altunakar (2007) with permission from Wiley Books.

2.2.3.2 Pressure effect on MSI

Pressure also has an effect on the a_w of a food system, but the effect is small compared with the temperature effect (Labuza and Albunakar, 2007). In most cases, the pressure effect can be neglected unless elevated pressures are used. According to Labuza and Albunakar (2007), the utility of a_w as a system descriptor under high pressure has not been demonstrated and methods of measurement have not been developed. The thermodynamic effect of pressure on water activity was discussed by Glasstone and Lewis (1960), who showed that a change in the total pressure of a system will affect the vapor pressure. The effect of pressure on a_w can be described by Eq. (2.7)

$$\ln \frac{a_{w2}}{a_{w1}} = \frac{\bar{V}_L}{RT}(P_2 - P_1) \tag{2.7}$$

where $\bar{V}_L$ is the molar volume of the liquid (water in this case); P_1 and P_2 are pressures for initial and final pressure, respectively.

2.2.3.3 Combined temperature-pressure effect on MSI

In some cases, a_w is influenced by the combination effect of temperature and pressure. Depending on the severity of each factor, neglecting the pressure effect could be an effective solution; however, in some cases, the combined effect of temperature and pressure on moisture sorption isotherms is estimated by using Eq. (2.8) (Labuza and Albunakar, 2007):

$$\ln\frac{a_{w2}}{a_{w1}} = \frac{-q_{st}}{R}\left[\frac{1}{T_2} - \frac{1}{T_1}\right] + \frac{\bar{V}_L \Delta P}{RT_2} \tag{2.8}$$

2.2.4 Mathematical description of MSI

To obtain basic information, such as some energy terms related to the level of interaction between water and food molecules, MSI needs to be described mathematically. Although there are about 77 different equations with varying degrees of fundamental validity (Bruin and Luyben, 1980; Rao et al., 2014), none provide accurate results in the full range of water activity for all types of food products (Al-Muhtaseb et al., 2002). The reason is that the water is associated in the solid food matrix with different mechanisms in different a_w regions (Labuza, 1974, Azuara and Beristain, 2006).

The equations used most commonly to describe MSI are BET (Brunauer, Emmett, and Teller) and GAB (Guggenheim, Anderson and De Boer) equations. The two equations allow the calculation of the monolayer adsorbed water value (M_0), which is the amount of water needed to form a layer of molecules that cover the food surface (Labuza, 1974; Iglesia and Chirife, 1984; Al-Muhtaseb et al., 2002). M_0 is often stated to represent the moisture content at which the water attached to each polar and ionic group starts to behave as a liquid-like phase and corresponds with the optimal moisture content for stability of low-moisture foods (Bell and Labuza, 2000;

Labuza, 1980). However, one of the assumptions behind the BET theory and GAB is that the sorption of molecules occurs on a surface whose structural and chemical characteristics are uniform, and that there are no lateral interactions between the molecules sorbed, which is not valid due to the heterogeneity of food materials (Nieto, 2010). Among the large number of models available, the equations that were used in this research are discussed below. These equations were selected because they have been shown to display a good fit for animal protein products (Basu, Shivhare and Mujumdar, 2006; Delgado and Sun, 2001).

2.2.4.1 Different isotherm equations

The Brunauer-Emmett-Teller (BET) equation

The BET equation (Brunauer, Emmett, and Teller, 1938) is used to fit MSI data over the range 0.05<aw<0.35-0.5 (Chirife and Iglesias, 1984). It provides an estimate of the monolayer value of moisture adsorbed on the surface and has been approved by the commission on Colloid and Surface Chemistry of the IUPAC (International Union of Pure and Applied Chemistry) (IUPAC, 1985) for standard evaluation of monolayer and specific area of sorbates. The BET equation can be written as Eq. (2.9)

$$\frac{a_w}{M(1-a_w)} = \frac{1}{CM_0} + \frac{C-1}{CM_0}(a_w) \tag{2.9}$$

where M is the moisture content (kg/kg dry solid), the constants defined as $b=(C-1)/(M_0C)$ and $c=1/(M_0C)$ are obtained from the slope and intercept, respectively, of the straight line generated by plotting $a_w/(1-a_w)*M$ against a_w. Then, the value of monolayer can be obtained from $M_0=1/(b+c)$.

The Henderson equation

Henderson equation (Henderson, 1952) is one of the most widely used models and can be written as Eq. (2.10):

$$M = \left[\frac{\ln(1 - a_w)}{-A}\right]^{\frac{1}{B}} \tag{2.10}$$

where M is the moisture content (kg/kg dry solid) and A and B are constants. A linearized plot of $\ln[-\ln(1-a_w)]$ versus moisture content has been reported to give rise to three"localized isotherms," which do not necessarily provide any precise information on the physical state of water, as was originally thought (Henderson, 1952; Rockland, 1969).

The Oswin equation

Oswin (1946) developed an empirical model, which is a series expansion of Pearson's equation for sigmoid shaped curves (type II), and can be written as Eq. (2.11):

$$M = A\left(\frac{a_w}{1 - a_w}\right)^B \tag{2.11}$$

where M is the moisture content (kg/kg dry solid) and A and B are constants. This equation was used by Labuza et al. (1972) to relate the moisture contents of non-fat dry milk up to a_w=0.5.

The Guggenheim-Anderson-de Boer (GAB) equation

The three-parameter GAB equation derived independently by Guggenhem (1966), Anderson (1946) and de Boer (1953) has been suggested to be the most versatile sorption model available in the literature. It represents a refined extension of Langmuir and BET theories, with three parameters having physical meanings. It can be written as Eq. (2.12):

$$M = ABC\frac{a_w}{(1 - Ba_w)[1 + (A - 1)Ba_w]} \quad (2.12)$$

where M is the moisture content (kg/kg dry solid) and A, B and C are constants.

The Halsey-Iglesias and Chirife (H-IC) equation

Iglesias and Chirife (1976b) simplified the original Halsey equation and H-IC equation can be written as Eq. (2.13):

$$M = \left[-\frac{A}{\ln(a_w)}\right]^{\frac{1}{B}} \quad (2.13)$$

where M is the moisture content (kg/kg dry solid) and A and B are constants. Iglesias, Chirife and Lombardi (1975) and Iglesias and Chirife (1976b) reported that the Halsey equation could be used to describe 220 experimental sorption isotherms of 69 different foods in the range of $0.1<a_w<0.8$. Sorption behavior of dried milk products (Linko, Pollari, Harju and Heikonen, 1982) have been well described by this equation.

The Hailwood and Horrobin equation

Hailwood and Horrobin (1946) generated a simple model to describe the absorption of water by polymers. Hailwood and Horrobin equation can be written as Eq. (2.14):

$$M = \left(\frac{A}{a_w} + B - Ca_w\right)^{-1} \quad (2.14)$$

where M is the moisture content (kg/kg dry solid) and A, B and C are constants.

The Iglesias and Chirife equation

Iglesias and Chirife (1976c) modified Fenkel-Halsey-Hill equation empirically and the equation can be written as Eq. (2.15)

$$a_w = \exp(-e^{AT+B} M^{-C}) \tag{2.15}$$

where M is the moisture content (kg/kg dry solid) and A, B and C are constants.

2.2.4.2 Calculation of the net isosteric heat of sorption from MSI

The net isosteric heat of sorption (q_{st}) (also called excess heat of sorption) can be calculated by Eq. (2.6). The isosteric heat of sorption was determined from the slope after plotting ln(a_w) versus 1/T at constant moisture content. This approach assumes that isosteric heat of sorption does not change with temperature. Accurate estimation of q_{st} using Eq. (2.6) requires measurement of water activities at several temperatures in the range of interest although a minimum of only two temperatures are needed.

Fig. 2.6 shows the behavior of the isosteric heat of sorption as a function of moisture content for desorption of water from pear (Iglesias and Chirife, 1976a). The plot shows the characteristic sharp decline in q_{st} with increasing moisture. The slope of the line (q_{st}/R) decreases to zero as moisture content increases. This is indicative of reduced water interactions (less binding energy) with the surface for adsorption, behaving more like pure water. The effect of temperature with respect to moisture content is shown to be the greatest at low moisture contents (Labuza and Albunakar, 2007).

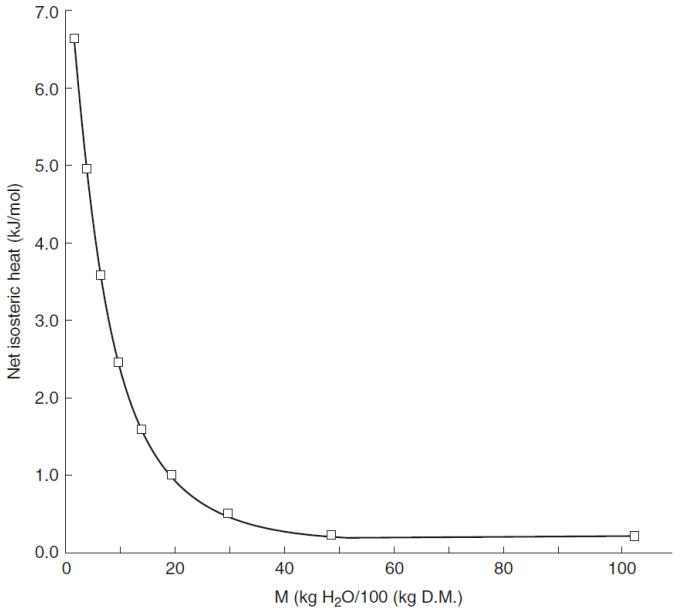

Figure 2.6. Net isosteric heat of sorption (q_{st}) for pear at 20 ˚C. Reprinted from Iglesias and Chirife (1976a) with permission from Taylor and Francis.

2.3 Effects of HPCD treatment on physicochemical properties of meat products

To date, the literature focusing on the effects of HPCD treatment on the physicochemical properties of meat products is quite limited (Wei, Balaban, Fernando and Peplow, 1991; Sirisee, 1998; Meurehg and Arturo, 2006; Choi et al., 2008; Ferrentino and Spilimbergo, 2011; Choi et al., 2013; Cappelletti, Ferrentino and Spilimbergo, 2015; Rahman, Seo, Choi, Gul and Yang, 2018). In this section, HPCD treatment's influence on meat color and texture is summarised. HHP treatment effects are also included for comparison purposes to help understand the influences of high pressure and HPCD.

2.3.1 Factors that influence meat color

Wei et al. (1991) reported a change in the color of chicken meat and shrimp, which turned whitish after HPCD treatment. Sirisee et al. (1998) found that ground beef looked like cooked ground beef after HPCD treatment. Brown and Mebine (1969) stated that high

concentration of CO_2 could cause darkening in meat tissues by combining with myoglobin to form metmyoglobin. Choi et al. (2008; 2013) found an increased lightness and lower redness value of meat following HPCD treatment. To explain the effect of HPCD on meat color, Choi et al. (2008) investigated the denaturation of the porcine muscle proteins with HPCD treatment. HPCD treatment had no effect on myofibrillar protein solubility, including myosin, while the SDS-PAGE analysis revealed denaturation of sarcoplasmic proteins (phosphorylase b, creatine kinase, triosephosphate isomerase and one unknown protein), which masked the red color of the sarcoplasm, causing the muscle to become pale. Cappelletti et al. (2015) stated that the HPCD treatment of raw pork meat resulted in an increase in lightness, decrease in redness, and the sample turned whitish and looked like "cooked" meat.

HHP treatment was also reported to lead to modifications of meat color (Szerman et al., 2011; Rodrigues et al., 2016). According to Marcos and Mullen (2014), HHP treatment induced strong modification of protein solubility and sarcoplasmic proteins ($p<0.001$) were more susceptible to HHP effect than myofibrillar proteins ($p>0.05$) in beef muscle proteome. Ferrini, Comapossada, Arnau and Guo (2012) found that the changes in the color of cured meat products depended on the water content and a_w. Ferrini et al. (2012) stated that HHP treatment increased *L* and reduced *a* and *b* values in raw cured ham with high water content but the effects were negligible on the low water content sample.

2.3.2 Factors that influence meat texture

Meurehg (2006) found the tenderness of ground beef to be higher after HPCD treatment. Choi et al. (2008) showed that HPCD treatment did not have an effect on the tenderness of porcine muscle. Choi et al. (2013) also found that HPCD treatment improved meat tenderness

when samples were treated at a relatively low pressure and temperature (150 bar and 31.1 ˚C) in comparison to the HHP treatment (3000 bar). Choi et al. (2013) reported that treated hot-pepper paste marinated pork samples were significantly more tender than the control samples ($p<0.05$). The majority of the studies showed that HHP treatment is associated with the tenderizing of meat due to structural changes of the myofibrils (Schumann et al., 1982; Suzuki et al., 1992; Cheftel and Culioli, 1997). Suzuki et al. (1992) reported that bovine semitendinosus muscle became more tender when pressurized to 3000 bar at 10 ˚C.

For both color and texture, the extent of the changes observed depends on the processing parameters (temperature, pressure, and time) applied, and the specific products used. More research is needed to better understand and minimize these changes during processing, especially for low a_w products.

Chapter 3: Effects of high pressure and CO_2 environment on the moisture sorption isotherm of beef jerky

3.1 Introduction

Beef jerky has been used for centuries as a processed dried meat product. The typical a_w range of the beef jerky products on the market is 0.77-0.82. High pressure carbon dioxide (HPCD) treatment is well known as a low temperature pasteurization technique but mainly for high a_w foods. It has been shown to be effective for microbial reduction in meat products, including chicken (Wei, Balaban, Fernando and Peplow, 1991) and ground beef (Sirisee, Hsieh, and Huff, 1998). In addition, an extended shelf life can be achieved without sacrificing nutritional and organoleptic quality of food since it is performed at relatively low temperatures. However, there are also some drawbacks associated with this technology, including the lack of a clear understanding of the microbial inactivation mechanism especially under low a_w environment, extraction of some food components, the need for high pressure equipment and the need for optimization of processing conditions for each case, depending on the type of food product and the type of microorganism targeted (Garcia-Gonzalez et al., 2007). Several studies (Haas et al., 1989; Nakamura, Enomoto, Fukushima, Nagai and Kakoda, 1994; Kumagai, Hata and Nakamura, 1997; Schmidt, Beermann, Bach and Schollmeyer, 2005) have shown that inactivation efficiency is reduced when HPCD is applied to low a_w food products.

Because moisture plays a critical role in microbial inactivation by HPCD treatment, it is necessary to understand the moisture sorption behavior in a CO_2 environment; however, the literature lacks information in this aspect. Moisture sorption isotherm (MSI) is a graphical expression of the relationship between total moisture content (MC) and the a_w of a food product

at a constant temperature and pressure within a defined surrounding atmosphere, typically air. MSI can be used to study the thermodynamics of water adsorption on a food material via measurement and modeling of the sorption isotherm. Comprehensive reviews on sorption behavior in foods and widely used mathematical sorption models have been published previously (Rizvi, 1986; Bell and Labuza, 2000; Al-Muhtaseb, McMinn, and Magee, 2002; Basu, Shivhare, and Mujumdar, 2006; Iglesias, 2012). However, how the MSI is affected in a CO_2 environment has not been reported even though such information would be valuable for further understanding of microbial inactivation mechanism during HPCD treatment of low a_w products. Therefore, the objective of this study was to determine the experimental data of MSI for beef jerky under different conditions: 1) air atmosphere at 23, 35, and 45 ˚C; 2) CO_2 atmosphere at 23 and 45 ˚C; and 3) high pressure CO_2 atmosphere at 45 ˚C and 57 bar and 200 bar. MSIs were generated by fitting experimental data into different mathematical models. Finally, the amount of monolayer of adsorbed water (M_0) for each isotherm and the net isosteric heat of sorption (q_{st}) were calculated.

3.2 Materials and methods

3.2.1 Materials

The beef jerky sample used in this study was prepared in the meat wing in Agri-Food Discovery Place located in the south campus of the University of Alberta. Two beef inside rounds were obtained from a federally inspected facility. Frozen beef stored at -20 ˚C was thawed in a cooler until slightly frozen. Then, beef was cut into 6 mm thick slices with a Berkel Model X13 meat slicer (Berkel, Chicago, IL, USA) at a speed setting of 30. Sliced beef was marinated overnight at 4 ˚C with cover brine, which consisted of beef jerky seasoning (without

monosodium glutamate) (Unipac, Edmonton, AB, Canada) and cure COOAE1 (Newly Weds Foods, Chicago, IL, USA) added according to the manufacturer's recommendations for the preparation of a marinated product. Marinated beef slices were placed on racks and transferred into a processing oven and smokehouse (ALKAR-RapidPak Inc., Lodi, WI, USA). Table 3.1 shows the treatment conditions used in the preparation of beef jerky. Sample a_w was measured 0.5 h after the first hour to get a final a_w of around 0.75 with Aqualab CX-2 water activity meter (Aqualab by Meter, Pullman, WA, USA). Finally, beef jerky samples were double bagged in 3 mm and 4 mm vacuum bags (Unipac, Edmonton, AB, Canada) with 5 slices per bag and sealed using a vacuum packager (Multivac Inc., Model C200, Kansas, MO, USA). Packed samples were stored at 0 ˚C until further use.

Table 3.1. Treatment conditions used for beef jerky processing.

Step	Step Time	DB Temp. (˚C)	WB Temp. (˚C)	%RH	Exhaust Fan	Exhaust Damper	Smoke Preheat
Cook	00:30	35	25	45	On	Auto	10
Smoke cook	01:00	35	24	40	Off	Closed	---
Smoke cook	01:00	45	29	30	Off	Closed	---
Cook	01:00	55	34	25	On	Auto	---
Cook	02:00	80	48	20	On	Auto	---

DB, dry bulb T; WB, wet bulb T; RH, relative humidity.

3.2.2 Proximate analysis

Proximate analysis was performed on the beef jerky sample to determine its protein, fat, water and ash contents. All measurements were performed in triplicate.

3.2.2.1 Protein content

The total protein content was determined by the Dumas combustion method (Buckee, 1994). A beef jerky sample (0.1±0.02 g) was sealed into a pellet, and the nitrogen content was measured with a TruSpec CN analyzer (Leco Corp., St Joseph, MI, USA). The protein content was calculated by multiplying the total nitrogen content with the conversion factor of 6.25.

3.2.2.2 Fat content

Total fat content was analyzed according to Hara and Radin (1978) with some modifications. A beef jerky sample (0.5±0.05 g) was chopped into small pieces and mixed with 10 mL hexane in a 16 mm * 125 mm screw cap culture tube. The samples were allowed to sit for 24 h in a fume hood with occasional shaking to ensure complete extraction of the fat. Then, the supernatant was transferred into a pre-weighed tube, dried under a gentle stream of nitrogen and weighed before and after drying.

3.2.2.3 Moisture content

The MC was determined according to the AOAC method 3.003 (AOAC, 1984). A beef jerky sample (0.5±0.05 g) was dried in an oven (Model 655G, Isotemp Oven, Fisher Scientific, Ottawa, ON, Canada) at 105 ˚C for 1 day. To generate MSIs, it is standard practice to express moisture content on dry basis, which was calculated using the following equation (Eq. 3.1):

$$MC\% = \frac{(Fresh\ sample\ weight - Dried\ sample\ weight\ )}{Dried\ sample\ weight} * 100\% \quad (3.1)$$

3.2.2.4 Ash content

The ash content was determined according to the AOAC method 7.009 (AOAC, 1984). A beef jerky sample (0.5±0.05 g) was burnt in a muffle furnace (Barnstead/Thermolyne® Muffle Furnace, Waltham, MA, USA) at 550 ˚C to constant weight. The ash content was calculated using the following equation (Eq. 3.2):

$$Ash\ \% = \frac{Burnt\ sample\ weight}{Fresh\ sample\ weight} * 100\% \quad (3.2)$$

3.2.3 Moisture sorption isotherm generation

In this study, a_w measurement method as described in Chapter 2 (section 2.2.2) was used to generate the MSI for beef jerky. All experiments were performed in triplicate. First, beef jerky was cut into 2.3*0.9*0.3 cm pieces and heated at 60 ˚C for 24 h resulting in dry beef jerky (a_w = 0.1 ± 0.05).

A glass container (20*16*8 cm) with a tight lip was filled to half height with distilled water so that the overhead space could generate a 100% relative humidity atmosphere. The dry beef jerky samples were placed in the overhead space in the glass container without any contact with water. The system was maintained at different temperatures (T=23, 35, 45±1 ºC) by placing the glass containers in ambient conditions (23 ˚C) or in an oven (Model 655G, Isotemp Oven, Fisher Scientific, Ottawa, ON, Canada) set at 35 or 45 ˚C. The samples were removed from the container at different time intervals (up to 65, 50, 25 h at 23, 35, 45 ˚C, respectively) so that they would adsorb different amounts of water. Then, the treated sample was stored in a refrigerator (~4 ˚C) for one week to allow the moisture to distribute uniformly throughout the sample. Finally, the a_w of the sample was determined using a water activity meter (Aqualab by Meter, Pullman,

WA, USA) at the same temperature of the treatment applied and the moisture content was determined as described above (section 3.2.2.3).

For those treatments performed in a CO_2 environment and ambient pressure, CO_2 atmosphere was created in the glass container by filling the overhead space with CO_2 gas, and the remaining steps were kept the same with treatment times of up to 40 and 20 h at 23 and 45 ˚C, respectively.

For those treatments performed under high pressure CO_2 environment, a phase equilibrium apparatus (SITEC-Sieber Engineering AG, Maur/Zurich, Switzerland) was used for creating the HPCD environment and the schematic diagram of the experimental apparatus is shown in Fig. 3.1. The apparatus mainly consisted of a 10 mL high pressure view cell connected to an ISCO 500D syringe pump (Teledyne Isco, Lincoln, NE, USA). A heating jacket was used to regulate the cell temperature, which was filled with circulating water connected to a water bath (Model 260, Thermo Fisher Scientific Inc., Waltham, MA, USA). A micrometering valve was connected to the exit to depressurize the vessel.

The cell was pre-heated to 45 ˚C. To create a high relative humidity environment in the cell, 500 μL water was added to the cell. The amount of added water was determined based on the solubility of water in CO_2 at the targeted temperature and pressure conditions to ensure saturation of CO_2 and to create 100% relative humidity environment in the cell (Wang et al., 2018). In addition, the added liquid water did not contact the beef jerky sample and expansion of liquid water phase within the HPCD environment was taken into consideration (Zhao et al., 2015). Custom designed glassware with holes at the bottom was used to hold the beef jerky sample to avoid contact with water in the bottom while allowing CO_2 circulation around the

sample. Then, the dried sample was placed into the cell followed by sealing the cell with its lid. The pre-heated cell (45 ˚C) was pressurized to the desired pressure (57 or 200 bar) with CO_2 and the magnetic stirrer was turned on. The dried sample was kept in the cell set at the desired temperature and pressure for different periods of time (up to 45 h at 57 bar; up to 9 h at 200 bar). Finally, the cell was depressurized at a rate of 60 bar/min. Treated samples were sealed and stored in a refrigerator for one week to allow the moisture to distribute uniformly throughout, prior to determination of a_w and MC.

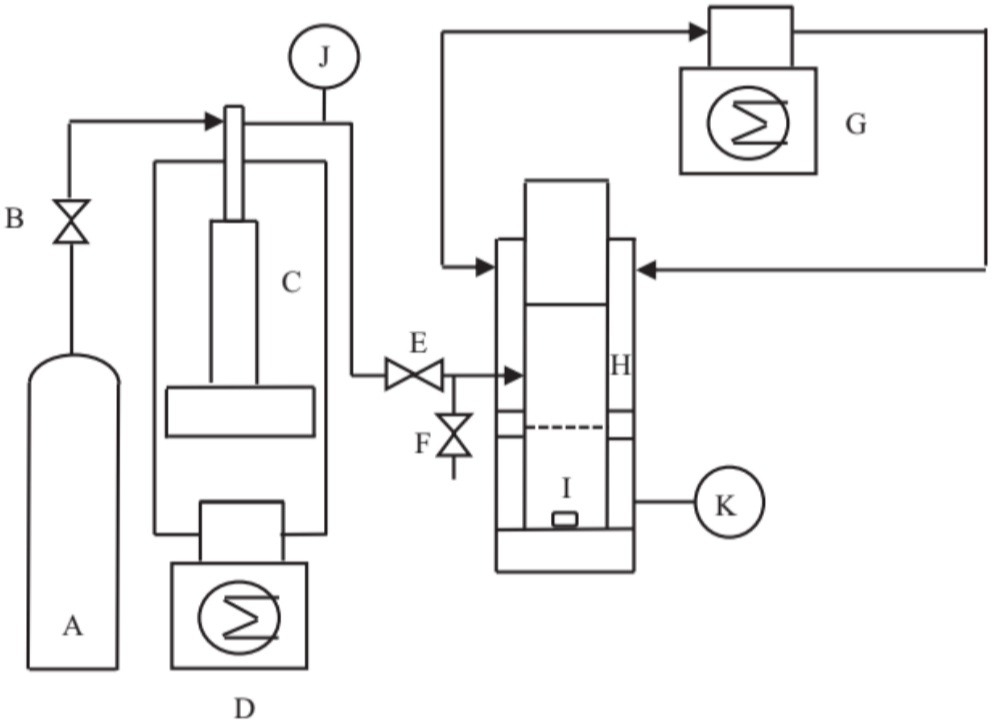

Figure 3.1. Schematic flow diagram of the high pressure system. (A) CO_2 tank; (B and E) on/off valves; (C) ISCO syringe pump; (D) refrigeration bath; (F) micrometering valve; (G) water bath; (H) high pressure view cell; (I) magnetic stirrer; (J) pressure gauge; (K) thermocouple.

3.2.4 Mathematical modelling

The experimental data were fitted to the moisture sorption isotherm equations (Eqs. (3.3)-(3.8)) shown in Table 3.2. A non-linear regression analysis was used to calculate the best value of the constants in each equation using the R software (R Core Team, 2018). All data points represent means of triplicate tests. The goodness of fit was evaluated by a mean relative percentage deviation (E) (Eq. 3.9) between the predicted (Mp_i) and experimental (M_i) moisture content values. Coefficient of determination (R^2) for best fit equation was also determined.

Table 3.2. Moisture sorption isotherm equations used for fitting experimental data.

Model	Equation	
Oswin (1946)	$M = A\left(\frac{a_w}{1-a_w}\right)^B$	(3.3)
Halsey-Iglesias and Chirife (H-IC) (1976b)	$M = \left[-\frac{A}{\ln(a_w)}\right]^{\frac{1}{B}}$	(3.4)
Hailwood and Horrobin (HH) (1946b)	$M = \left(\frac{A}{a_w} + B - Ca_w\right)^{-1}$	(3.5)
Guggenheim (1966), Anderson (1946) and de Boer (1953)-(GAB)	$M = ABC\frac{a_w}{(1-Ba_w)[1+(A-1)Ba_w]}$	(3.6)
Henderson (1952)	$M = \left[\frac{\ln(1-a_w)}{-A}\right]^{\frac{1}{B}}$	(3.7)
Iglesias and Chirife (IC) (1976c)	$a_w = \exp(-e^{AT+B}M^{-C})$	(3.8)

M is the moisture content (dry basis); A, B, C are constants; and T is temperature in ˚C.

$$E = \frac{100}{n}\sum_{i=1}^{n}\frac{|M_i - Mp_i|}{M_i} \quad (3.9)$$

3.2.5 Determination of monolayer water content (M_0)

The monolayer water content (M_0) was obtained from Brunauer, Emmett and Teller (BET) plots (Brunauer, Emmett, and Teller, 1938). The linearized form (Eq. 3.10) of this isotherm was plotted in terms of a_w. This function was applied within the linear range of the isotherm (a_w<0.5).

$$\frac{a_w}{M(1-a_w)} = \frac{1}{CM_0} + \frac{C-1}{CM_0}(a_w) \quad (3.10)$$

Finally, M_0 was calculated from the slope (S) and intercept (I) of the line $a_w/M(1-a_w)$ as a function of a_w according to Eq. (3.11).

$$M_0 = \frac{1}{I+S} \quad (3.11)$$

The M_0 results obtained under the seven conditions tested were analyzed by one-way analysis of variance (ANOVA), and multiple comparison of the means was performed using the Tukey's test at a significance level of p<0.05.

3.2.6 Determination of net isosteric heat of sorption (q_{st})

Net isosteric heat of sorption (q_{st}) was calculated at different moisture content levels by using the Clausius-Clapeyron equation (Eq. 2.6) (section 2.2.3.1), employing the MSIs obtained at 23 and 45 ˚C in air and CO_2 atmospheres at 1 bar.

3.3 Results and Discussion

3.3.1 Composition of beef jerky

The proximate composition of the beef jerky samples used in this study are presented in Table 3.3.

Table 3.3. Chemical composition of beef jerky samples.

Composition	%, w/w*
Protein	47.65±0.49
Fat	2.04±0.89
Moisture	38.07±2.69
Ash	12.49±0.010

***** Mean±standard deviation based on triplicate analysis.

3.3.2 Moisture sorption isotherms

The experimental data points of MSIs are presented in Fig. 3.2 together with the curves obtained by using the best fitted model for each data set.

3.3.2.1 Mathematical modeling of the moisture sorption isotherms

Eqs. (3.3)-(3.8) were used to fit the MSI for beef jerky sample. The mean relative percentage deviation (E) for the different models is reported in Table 3.4. An equation is considered a good fit for data when E<10. Table 3.5 shows the parameters of the best fit equations for beef jerky MSIs at each condition, and the R^2 values for the best fit equations.

Table 3.4 shows that under air atmosphere and ambient pressure, HH and GAB models gave the best fit of experimental MSI data at 23 ˚C; GAB provided the best fit at 35 ˚C; and IC fit 45 ˚C data the best. However, none of these models gave a good fit (E>10) for the

experimental data under CO_2 atmosphere either at ambient pressure or high pressure with *E* values reaching as high as 80. This finding highlights the need for additional research to improve the available models to describe MSI data obtained under CO_2 atmosphere better.

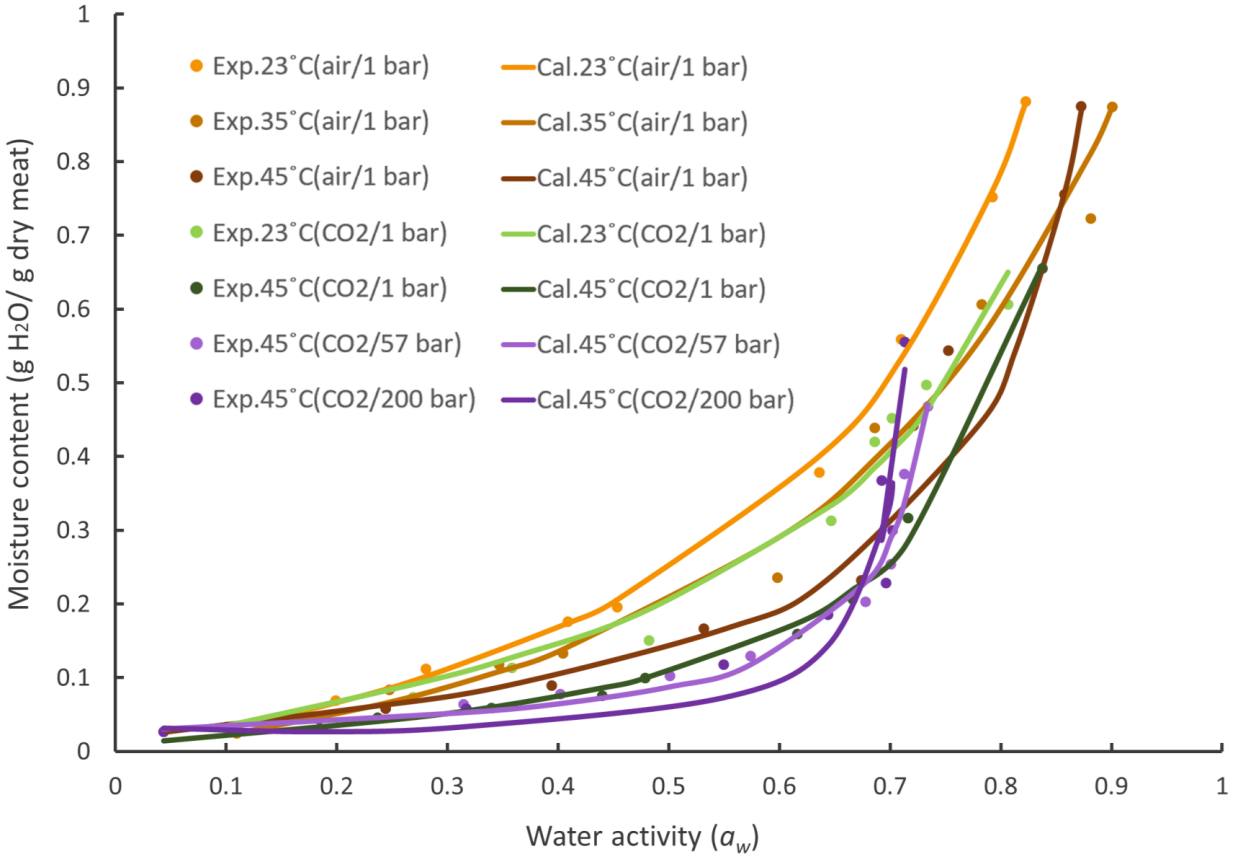

Figure 3.2. Moisture sorption isotherms of beef jerky under different conditions (n=3). The following curves were obtained using the GAB model (Eq. (3.6)): 23 ˚C (air/1 bar); 35 ˚C (air/1 bar); 45 ˚C (CO_2/57 bar); the curve for 45 ˚C (air/1 bar) was obtained using the IC model (Eq. (3.8)); the curve for 23 ˚C (CO_2/1 bar) was obtained using the Oswin model (Eq. (3.3)); the curve for 45 ˚C (CO_2/1 bar) was obtained using the H-IC model (Eq. (3.4)); the curve for 45 ˚C (CO_2/200 bar) was obtained using the HH model (Eq. (3.5)).

Table 3.4. Accuracy of fit of different models expressed as mean relative percentage deviation (*E*).

		Oswin	H-IC	HH	GAB	Henderson	IC
Air/1 bar	23˚C	5.17	19.48	4.67	4.67	12.81	40.99
	35˚C	34.55	53.42	11.89	9.37	11.94	12.82
	45˚C	21.44	27.68	26.28	13.76	23.24	6.03
CO_2/1 bar	23˚C	11.72	23.74	14.93	13.60	12.77	56.94
	45˚C	20.04	10.92	19.05	19.04	30.34	80.04
HPCD/45˚C	57 bar	36.11	32.41	12.17	12.16	39.30	81.15
	200 bar	51.79	50.06	27.54	77.71	52.92	79.91

Table 3.5. Parameters of the best fit equations for beef jerky.

		Best fit equation	A	B	C	R^2
Air/1 bar	23 ˚C	HH	3.6321	2.9841	0.3576	0.998
	23 ˚C	GAB	0.26631	1.11439	0.92773	0.998
	35 ˚C	GAB	13.8122	0.022494	0.62172	0.981
	45 ˚C	IC	0.00633	-2.06049	0.87631	0.980
CO_2/1 bar	23 ˚C	Oswin	0.20435	0.81148	N/A	0.975
	45 ˚C	H-IC	-0.12946	0.75489	N/A	0.995
HPCD/45 ˚C	57 bar	GAB	0.03214	158.9	1.269	0.977
	200 bar	HH	-0.9234	56.375	74.5234	0.902

According to Brunauer, Deming, Deming and Teller (1940), sorption isotherms are classified into 5 types as described in Chapter 2 (section 2.2.1). The MSIs under ambient pressure in both air and CO_2 environments showed sigmoid (type II) characteristics, but under HPCD condition the isotherms changed to type III as discussed below. Comaposada, Gou, Pakowski and Arnau (2000) used the Mujica model to describe a type III isotherm. However, use of the Mujica model for the MSIs obtained in this study did not improve the *E* value.

3.3.2.2 Effect of temperature

Isotherms of the beef jerky at 23, 35 and 45 ˚C in air at ambient pressure are shown in Fig. 3.2. The MC decreased as temperature increased at a given a_w. Similar observations were also reported by Igobeka and Blasidell (1982) for a meat product, and Delgado and Sun (2001) on cooked and cured beef. According to Palipane and Driscoll (1992), and Hossain, Bala, Hossain and Mondol (2001), as temperature increases, water molecules move to higher energy levels, which results in water molecules breaking away from water binding sites on the solid particles. Therefore, at a constant MC, the a_w increased with temperature, indicating a decrease in bound water and an increase in the level of free water. A similar trend was also apparent in CO_2 atmosphere at ambient pressure with increasing temperature.

3.3.2.3 Effect of CO_2 and HPCD environment

When the isotherms obtained under air and CO_2 atmospheres at 23 ˚C and ambient pressure were compared (Fig. 3.2), the MC at a given a_w was lower in CO_2 atmosphere; however, at 45 ˚C, the two isotherms were very close and even overlapped in the high a_w range. According to Jakobsen and Bertelsen (2002), CO_2 can be adsorbed onto proteins so that there would be less surface available for water adsorption and therefore less water was adsorbed to achieve similar a_w at 23 ^oC. However, at 45 ^oC, with increased volatilization of CO_2, less CO_2 would be adsorbed onto the proteins, diminishing the difference between the isotherms obtained in CO_2 and air atmospheres. In addition, the solubility of CO_2 in muscle tissue decreases with increasing temperature (Jakobsen and Bertelsen, 2002), which explains the smaller gap between the two isotherms (under air and CO_2 environment at ambient pressure) at the higher temperature of 45 ˚C.

Under HPCD conditions, the isotherms became very steep (J-like shape) at a_w level of 0.73 and 0.70 at 57 and 200 bar, respectively (Fig. 3.2). J-like shaped isotherms were also reported for osmotically dehydrated and smoked Atlantic bonito muscle (Hubinger, Vivanco-Pezantes, Kurozawa and Sobral, 2009), and cod fish (Martins, Martins and da Silva Pena, 2015). Products containing soluble crystalline components, e.g., salts, often have J-shape isotherms. The effect of soluble components on MSI was studied by other authors, including but not limited to Chinachoti and Steinberg (1984), Comaposada et al., (2000), and Martins et al. (2015). Comaposada et al. (2000) and Martins et al. (2015) observed that MSIs were stabilized at a level of 0.75 a_w, which is the a_w of a saturated NaCl solution at 25 ˚C (36 g NaCl/100 g H_2O) (Greenspan, 1977; Lioutas, Bechtel and Steinberg, 1984). According to Lioutas et al. (1984), the NaCl solution crystallises below water activity of 0.75, and the crystallised NaCl adsorbs little or no water. When a_w>0.75, a solution was produced by adsorbing a large amount of water rapidly with small increases in a_w. Therefore, the a_w of the inflection point is determined by the solubility of NaCl under different conditions. According to Gibson (1938), and Owen and Brinkley (1941), the solubility of NaCl in water increases with pressure while higher concentrations correspond to lower a_w. This could be one possible reason for the isotherms at high pressure CO_2 environment turning steep at a_w level of 0.73 and 0.70 at 57 bar and 200 bar, respectively. Martins (2015) reported that the isotherms of cod fish changed from type II to type III with an increase in salt content. On the other hand, Bando, Takemura, Nishio, Hihara and Akai (2003) demonstrated that the CO_2 solubility in water decreased with increasing NaCl concentration. Therefore, in the present study, HPCD treatment may have an effect on protein-salt bonding and make salt more available. As a result, the change in the shape of the isotherms showed similar behavior to that when there was an increase in salt content. Regardless,

further research is needed to better understand the changes in water-salt-protein-CO_2 interactions under high pressure.

3.3.3 Monolayer water content (M_0)

The results for determination of M_0 under different conditions were presented in Fig. 3.3. M_0 value decreased (p<0.05) with an increase in temperature but pressure did not have a significant effect (p>0.05). Different dehydrated food products show that M_0 decreases with increasing temperature (Chen and Clayton, 1971; Iglesias, Chirife and Lombardi, 1975; Al-Mahasneh, Alkoaik, Khalil, Fulleros and El-Waziry, 2014). According to Rao, Rizvi, Datta and Ahmed (2014), a reduction in the number of active sites due to chemical and physical changes induced by temperature is the reason for this behavior. In other words, samples with the same water content, would have more free water with an increase in temperature.

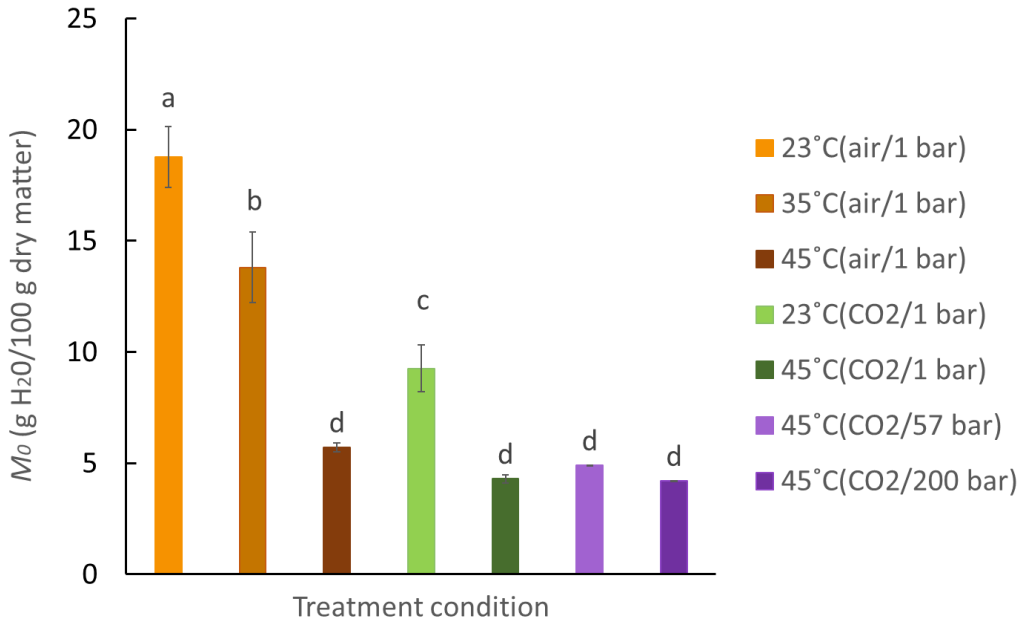

Figure 3.3. Monolayer water content (M_0) under different conditions (n=3). Bars with different superscripts are significantly different (p<0.05).

3.3.4 Net isosteric heat of sorption (q_{st})

Net isosteric heat of sorption (q_{st}) of beef jerky at 34 ˚C (average temperature between 23 and 45 ˚C) in air and CO_2 environments at ambient pressure as a function of moisture content is presented in Fig. 3.4. It is important to note that q_{st} plus latent heat of vaporisation of pure water makes up the total isosteric heat of sorption. Fig. 3.4 shows a comparison between the air and CO_2 environments, where the q_{st} value in CO_2 environment is higher and the differential between the two environments decreases when the moisture content is increased. The highest q_{st} value was 4,034 kJ/kg and 17,474 kJ/kg for beef jerky under air and CO_2 environments, respectively, at 10% moisture level and approached zero at the high moisture levels. The highest q_{st} value for cured beef obtained by Delgado and Sun (2002) was 3,780 kJ/kg, which is in agreement with the value obtained for beef jerky in this study. The decrease in the q_{st} with the increase in moisture content can be qualitatively explained by the fact that sorption initially occurs on the most active sites, giving rise to the greatest interaction energy, but as the moisture content increases, there are fewer sorption sites available for water, resulting in a lower value of q_{st} (Tsami, Maroulis, Marinos-Kouris and Saravacos, 1990).

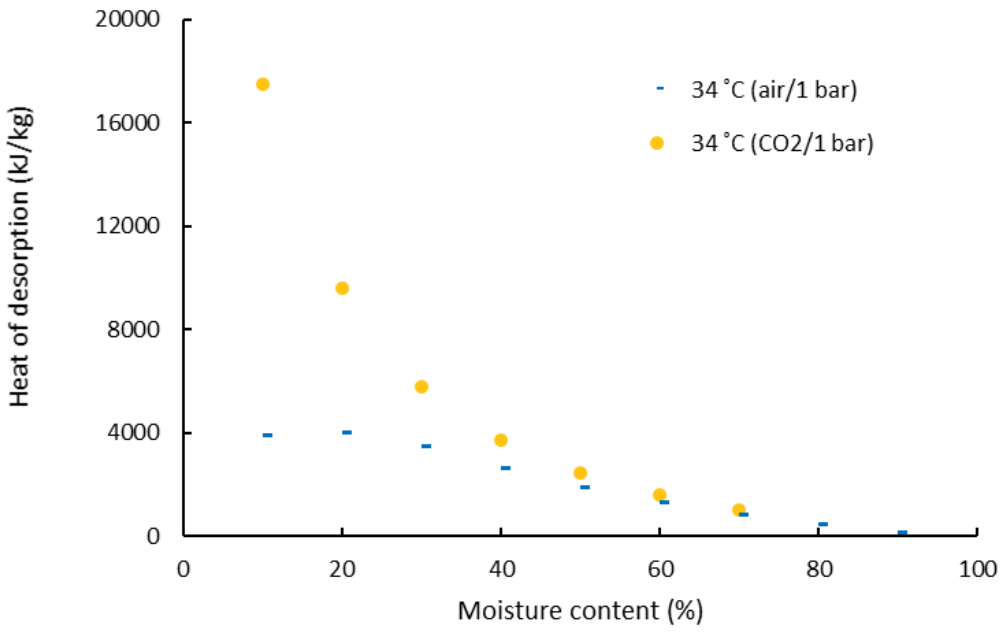

Figure 3.4. Net isosteric heat of desorption (q_{st}) of water in beef jerky under air and CO_2 environments at ambient pressure.

3.4 Conclusions

The influence of temperature, CO_2 atmosphere at ambient pressure and HPCD environment on MSIs of beef jerky was evaluated. The deviation of the mathematical models used to fit the data increased under CO_2 atmosphere at ambient pressure and HPCD conditions. With an increase in temperature and switching from air atmosphere to CO_2, the a_w increased at a given moisture content, indicating higher level of free water. However, under CO_2 atmosphere at high pressures of 57 and 200 bar, the isotherms became very steep at a_w of 0.73 and 0.70, respectively, displaying J-shaped, type III isotherms. Monolayer water content decreased with temperature, but pressure did not have a significant effect on M_0. Net isosteric heat of sorption in CO_2 environment was higher than that in an air environment and the differential between the two environments decreased when the moisture content was increased.

Chapter 4: Effect of high pressure CO_2 treatment on the physicochemical properties of beef jerky

4.1 Introduction

In recent years, there has been a growing demand for the minimally processed Ready-To-Eat (RTE) meat products, free of chemical additives (Decker and Park, 2010; Zhang, Xiao, Samaraweera, Lee and Ahn, 2010). Among the RTE meat products, beef jerky is a popular choice in North America and its consumption has increased by 20% from 2011 to 2018 in the USA (Statistica, 2019). However, safety of the final product depends on the quality of the raw beef material and contamination of the beef can happen during slaughter and processing (Wheeler, Kalchayanand and Bosilevac, 2014; McCarty, 2016).

High pressure CO_2 (HPCD) treatment has been known as a non-thermal process for extending the shelf-life and safety of RTE meat products due to its microbial inactivation effect. HPCD was shown to be effective at reducing specific bacteria, including *Listeria monocytogenes, Staphylococcus aureus* and *Escherichia coli*, in beef and other meat products (Wei, Balaban, Fernando and Peplow, 1991; Sirisee, Hsieh and Huff, 1998). However, HPCD treatment can affect the physicochemical properties of meat. For example, the color of chicken meat became whiter, while that of ground beef became darker with an increase in tenderness after HPCD treatment (Wei et al., 1991; Sirisee et al., 1998; Meurehg and Arturo, 2006). Nevertheless, there are only very limited reports to date on the effect of HPCD treatment on the physicochemical properties of meat and none specifically on beef jerky. Since the majority of the studies on HPCD treatment deals with high moisture products, it is also worthwhile to demonstrate its impact on the quality attributes of a product with a low water activity like beef jerky.

Therefore, the objective of this study was to investigate the combined effects of different HPCD processing parameters, including pressure (*P*), temperature (*T*), treatment time (*t*), and depressurization rate (*DR*), on the physicochemical characteristics of HPCD-treated beef jerky. Physicochemical characteristics evaluated in this study include water activity (a_w), surface color profile, crude fat content and Warner-Bratzler shear force (WBSF).

4.2 Materials and methods

4.2.1 Materials

The preparation of beef jerky was described in Chapter 3 (section 3.2.1).

4.2.2 HPCD treatment

Beef jerky was cut into 2.3*0.9*0.3 cm pieces so that it could fit into the high pressure treatment cell. The schematic diagram of the high pressure apparatus used for HPCD processing (Phase equilibria apparatus, SITEC-Sieber Engineering AG, Maur/Zurich, Switzerland) was presented in Chapter 3 (Fig. 3.1).

The unit was pre-heated to the desired temperature and the beef jerky sample was placed into the cell. The cell was sealed with its lid and pressurized to the desired pressure. Treatment time was started once the pressure reached the desired value. Treatment times reported in this study do not include pressurization and depressurization times. Finally, the cell was depressurized at different rates, *DR*, controlled manually by a micrometering valve.

4.2.3 Characterization of physicochemical properties

The following analyses were performed before and after the HPCD treatment under different conditions. All measurements were performed in triplicate.

4.2.3.1 Water activity

Sample a_w was determined by an Aqualab CX-2 water activity meter (Aqualab by Meter, Pullman, WA, USA) set at measurement temperature of 25 ˚C.

4.2.3.2 Surface color profile

Surface color was measured with the Chroma Meters CR-410 (Konica Minolta Sensing America Inc, Ramsey, NJ, USA). Color profile was presented by *L*, *a*, and *b* values. *L* represents lightness with *L*=0 referring to black and *L*=100 referring to white; *a* value going from low to high represents color change from green to red; and *b* value going from low to high indicates color change from blue to yellow.

4.2.3.3 Fat content

Total fat content was analyzed according to Hara and Radin (1978) with some modifications as described in Chapter 3 (section 3.2.2.2).

4.2.3.4 Warner-Bratzler shear force

WBSF was measured by shearing once through the centre of the beef jerky sample (2.3*0.9*0.3 cm) with a WBSF device attached to an Universal Instron apparatus (Model 5967, Instron Ltd, Buckinghamshire, UK) fitted with a 5k N tension/compression load cell at a crosshead speed of 200 mm/min. Force at rupture was recorded in Newtons (N).

4.2.4 Experimental design

4.2.4.1 Central composite rotatable design

A five-level, four-variable, central composite rotatable design (CCRD) was employed using a commercial statistical package, MINITAB version 18 (Minitab Inc., State College, PA, USA). The independent variables were pressure (*P*), temperature (*T*), treatment time (*t*), and depressurization rate (*DR*) and these variables were coded at levels of -1.414, -1, 0, +1, and +1.414. Uncoded and coded independent variables are given in Table 4.1. Design of experiments was based on coded levels of the independent variables in the CCRD, which resulted in 31 experimental runs, including 7 replications at the central point as shown in Table 4.2. Experiments were randomized to minimize the systematic bias in the observed responses due to extraneous factors and to increase precision.

Table 4.1. Uncoded and coded levels of independent variables used in the central composite rotatable design.

Coded variables	***P* [bar]**	***T* [˚C]**	***t* [min]**	***DR* [bar/min]**
-1.414	58.6	30.9	6.7	33.4
-1	100	35	15	50
0	200	45	35	90
+1	300	55	55	130
+1.414	341.4	59.14	63.28	146.56

Table 4.2. Central composite rotatable design with coded variables.

No. of experiments	*P*	*T*	*t*	*DR*
1	0	0	0	0
2	-1	-1	1	-1
3	-1	1	1	1
4	0	0	0	0
5	1	1	1	-1
6	0	-1.414	0	0
7	1	-1	-1	1
8	-1	1	-1	1
9	1	-1	1	1
10	-1	-1	1	1
11	-1	-1	-1	1
12	-1	-1	-1	-1
13	1	1	1	1
14	1	1	-1	1
15	1	-1	-1	-1
16	0	0	0	0
17	-1.414	0	0	0
18	0	0	0	0
19	1	1	-1	-1
20	0	1.414	0	0
21	0	0	1.414	0
22	0	0	0	0
23	-1	1	-1	-1
24	0	0	0	0
25	0	0	0	0
26	0	0	-1.414	0
27	1.414	0	0	0
28	1	-1	1	-1
29	-1	1	1	-1
30	0	0	0	-1.414
31	0	0	0	1.414

4.2.4.2 Fitting the model and data analysis

The data obtained from the experiments were analyzed by fitting a mathematical equation (Eq. 4.1) to describe the behavior of the responses according to the levels of studied values. With the objective of minimizing the quality changes due to HPCD treatment, the response variable used for modeling was the difference (ΔY, Eqs. 4.1 and 4.2) in the physicochemical properties determined (a_w, L, a, b, fat content, WBSF) between the treated and untreated samples. Least square method (LSM) was used to perform the regression analysis and determine the coefficients of Eq. (4.1). The achieved mathematical model was evaluated by the application of analysis of variance (ANOVA). The significance of each coefficient was assessed by p-value and model terms with $p<0.05$ were considered as significant.

$$\Delta Y = \beta_0 + \sum_{i=1}^{k} \beta_i X_i + \sum_{i=1}^{k} \beta_{ii} X_i^2 + \sum_i \sum_j^k \beta_{ij} X_i X_j + \in \quad (4.1)$$

$$\Delta Y = Y' - Y \quad (4.2)$$

where ΔY is the difference in responses between treated and untreated sample, Y' is the response of sample after HPCD treatment, Y is the response of sample before HPCD treatment, X_i X_j refer to coded process variables, β_0 is a constant, β_i, β_{ii} are the first and second degree coded input parameters, β_{ij} is the parameter for interactions of linear, quadratic and 2-way interaction terms, k is the number of independent parameters (k=4 in this study) and $\in$ is the error term.

4.2.4.3 Optimization of HPCD treatment conditions

The optimum condition was obtained by using the MINITAB software by targeting minimum changes in the four responses, which were weighted equally. The change in each response factor, comparing before and after HPCD treatment (ΔY), was minimized in the optimization function. For confirmation, samples were treated at the optimum condition and the responses (a_w, L, a, b, fat content, WBSF) were measured.

According to Schultze (2019), P=57 bar, T=65˚C, t=15 min, DR=60 bar/min with the addition of water was the condition that resulted in the best microbial inactivation using the same beef jerky sample. Therefore, additional HPCD treatments were performed under the condition defined by Schultze (2019) with and without the addition of 500 μL water and the responses were determined for comparison to the sample obtained under the optimum condition determined in this study.

4.2.5 Morphology analysis

Four samples (untreated, treated under the optimum condition obtained by MINITAB software, treated under the condition reported by Schultze (2019) without and with the addition of 500 μL water into the high pressure chamber) were prepared and their morphology was observed under a light microscope (ZEISS AXIO Scope.A1, Oberkochen, Germany).

4.3 Results

4.3.1 Fitting the model and analysis of experimental data

The results for the observed responses are summarized in Table 4.3. The experimental data in Table 4.3 were used to calculate the coefficients of the quadratic polynomial equation (Eq. (4.1)) by the LSM technique.

Table 4.3. Recorded ΔY response values.

No. of experiments	a_w	Surface color profile			Fat content (%)	WBSF (N)
		L	*a*	*b*		
1	-0.02343	1.0900	0.53666	1.2100	-0.638	17.6213
2	-0.00825	1.2948	0.36142	1.4225	-2.163	-14.3559
3	-0.03935	2.2889	0.16142	1.4650	-3.445	0.6579
4	-0.02823	0.8233	0.30333	0.7800	0.366	-5.1075
5	-0.02105	1.5723	0.29142	2.0175	-3.325	-4.1675
6	-0.02152	0.7405	0.58791	2.2183	-1.060	-19.6039
7	-0.02425	1.9072	0.25000	1.9250	-0.807	-11.3377
8	-0.02355	1.6500	0.42555	1.8319	-1.267	-3.0656
9	-0.00545	1.2723	0.26142	2.1525	-3.665	-8.6661
10	-0.02872	1.1905	0.37000	1.6138	-1.641	-13.3384
11	-0.01345	0.1223	0.34142	1.2425	-1.148	-16.3595
12	-0.01955	0.8516	0.17666	1.4016	-0.509	-10.7875
13	-0.02695	2.5100	0.49055	3.0344	-1.070	-1.8708
14	-0.04275	2.4773	0.27142	1.8275	-2.900	-13.3640
15	-0.01495	0.6898	0.35642	1.7000	-2.980	-0.2185
16	-0.03153	1.2533	-0.04333	0.8466	-2.799	7.2873
17	-0.02066	1.1283	0.22777	0.7183	-2.294	-8.8892
18	-0.03353	0.8233	0.30333	0.7800	-1.892	9.4921
19	-0.02825	2.7750	0.14555	1.5627	-0.905	-1.0332
20	-0.02765	2.9550	0.32555	2.6194	-2.178	8.9227
21	-0.01275	3.2527	0.28888	2.7494	-2.995	-10.7348
22	-0.03543	1.9200	0.25666	1.1600	-2.686	11.0696
23	-0.03155	2.0448	0.34476	1.5366	-2.767	1.8599
24	-0.04053	0.4233	0.23666	0.8966	-2.316	-8.3420
25	-0.04853	0.8961	0.45222	1.0261	-2.416	14.1964
26	-0.03153	1.1838	0.19444	1.2372	-2.385	-4.8852
27	-0.02973	2.0283	0.27777	1.6605	-2.224	1.6365
28	-0.02979	1.3527	0.34000	1.6383	-1.686	-17.3897
29	-0.02835	1.2866	0.19555	1.2294	0.175	-13.8393
30	-0.01708	2.2716	0.27222	1.7038	-2.424	-12.9828
31	-0.01329	1.6961	0.32555	2.4894	-1.083	-7.2968

4.3.1.1 Effect on a_w

The significance of each factor was determined by the standardized Pareto chart, as shown in Fig. 4.1. The length of each bar is proportional to the impact of each corresponding effect on the response. Any bar extending beyond the vertical line indicated that the variable is statistically significant at $p<0.05$. The results for a_w indicated that the linear T term was significant ($p<0.05$), whereas all the other first-order terms, quadratic terms and interaction terms did not have an effect on a_w. Therefore, the model was simplified to include only the significant terms and the regression coefficients of the predicted model for a_w are summarized in Table 4.4. The proposed mathematical model is shown in Eq. (4.3).

$$\Delta Y_{aw} = 0.1015 - 0.00287\ T \qquad (4.3)$$

The responses, ΔY for a_w obtained under different conditions were all negative, which indicated that the HPCD treatment resulted in a decrease in sample a_w. From Eq. (4.3), it can be seen that ΔY_{aw} decreases with an increase in treatment T.

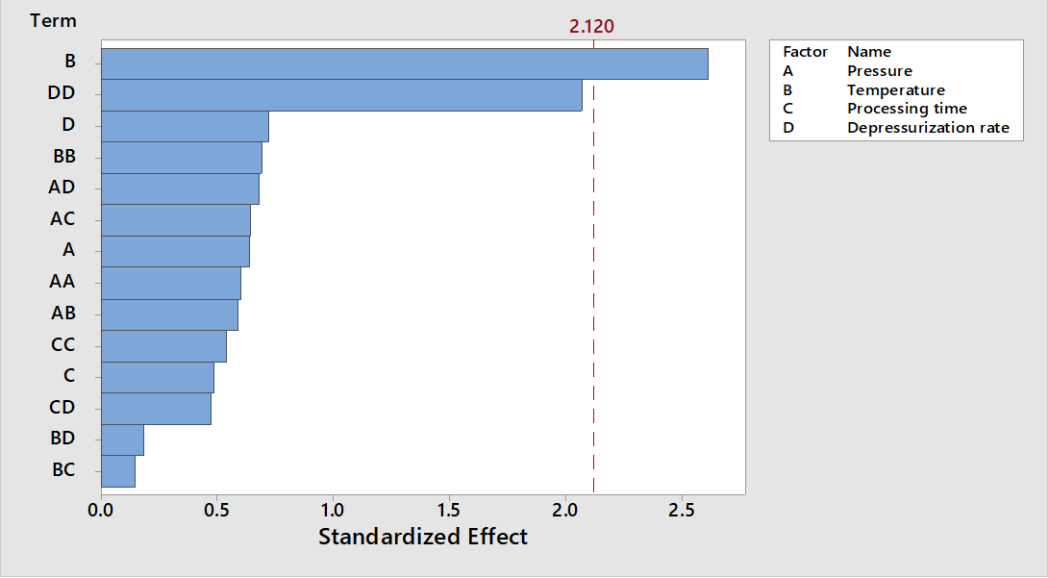

Figure 4.1. Pareto chart of the standardized effects for the response a_w (α=0.05).

Table 4.4. Regression coefficients of the model for a_w for coded coefficients.

Term	Coefficient	SE Coef.	P-Value
Constant	-0.03204	0.00353	0
T	-0.00613	0.00234	0.019

The fitted model was analyzed via the analysis of variance (ANOVA) as shown in Table 4.5. The model shows that the lack-of-fit error is insignificant, indicating that the fitted model is accurate enough to predict the response a_w.

Table 4.5. ANOVA for a_w model.

Source	DF	Adj SS	Adj MS	F-Value	P-Value
Model	14	0.001834	0.000131	1.2	0.363
T	1	0.00075	0.00075	6.85	0.019
Error	16	0.001754	0.00011		
Lack-of-Fit	10	0.001451	0.000145	2.88	0.104
Pure Error	6	0.000302	0.00005		
Total	30	0.003588			

Residual plots for a_w are shown in Fig. 4.2. The probability plot and histogram of residuals, Figs. 4.2 (a, c), can be used to verify the normality assumption. Therefore, ideally, a histogram chart displays a normal distribution. Fig. 4.2 (c) shows that the data somewhat resembled the normal distribution, except for the high frequency at -0.015 residual. Figs. 4.2 (b, d) show that the residuals fall in a horizontal band with no systematic pattern. This implies that the model proposed is adequate and there is no reason to suspect any violation of the independence or constant variance assumption.

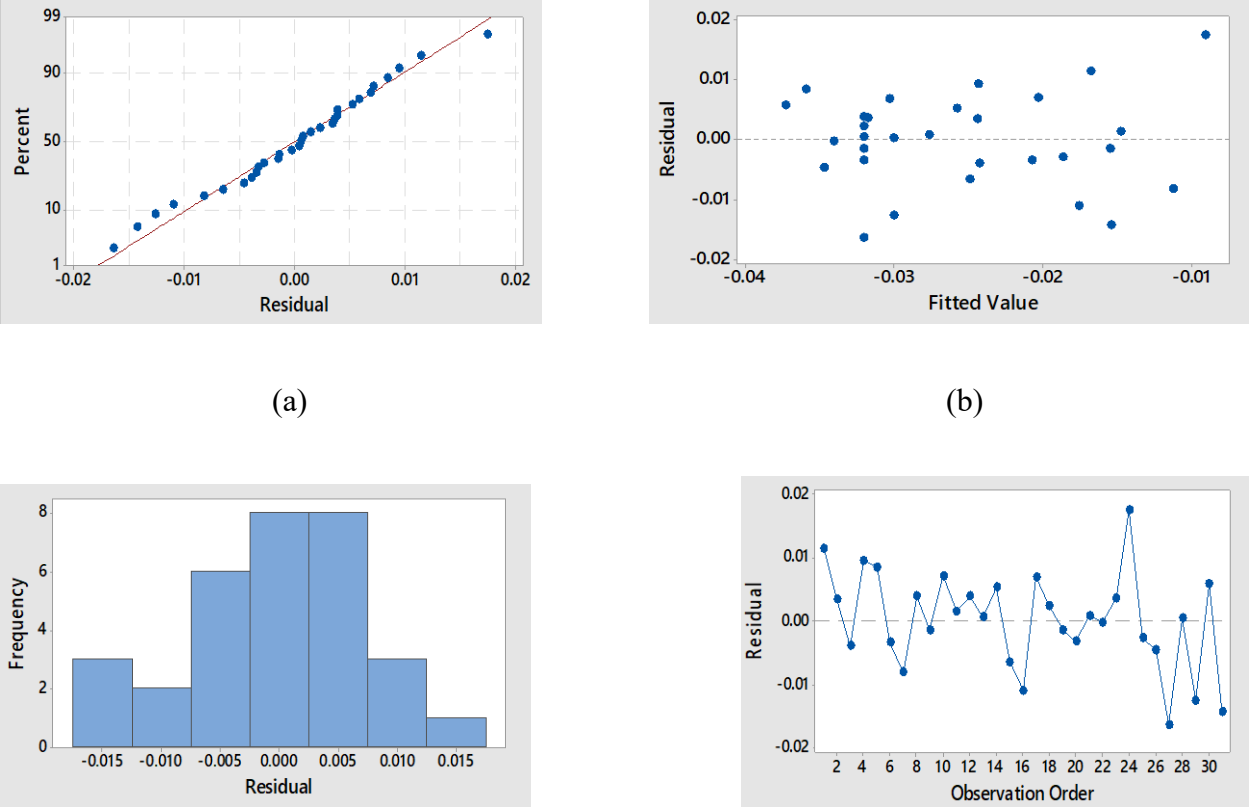

Figure 4.2. Residual plots for a_w: (a) Normal probability plot for standardized residuals, (b) versus fits for standardized residuals, (c) histogram of standardized residuals, and (d) versus order for standardized residuals.

4.3.1.2 Effect on surface color

Pareto charts for *L*, *a*, *b* values are shown in Figs. 4.3, 4.4, and 4.5, respectively. The results indicated that the linear *P* term was significant ($p<0.05$) on *L* whereas all the other first-order terms, quadratic terms and interaction terms had no effect on *L* value. None of the linear, quadratic or interaction terms showed any significant effect on *a* value. In terms of the *b* value, linear *P*, quadratic *P* and linear *DR* terms showed a significant ($p<0.05$) effect.

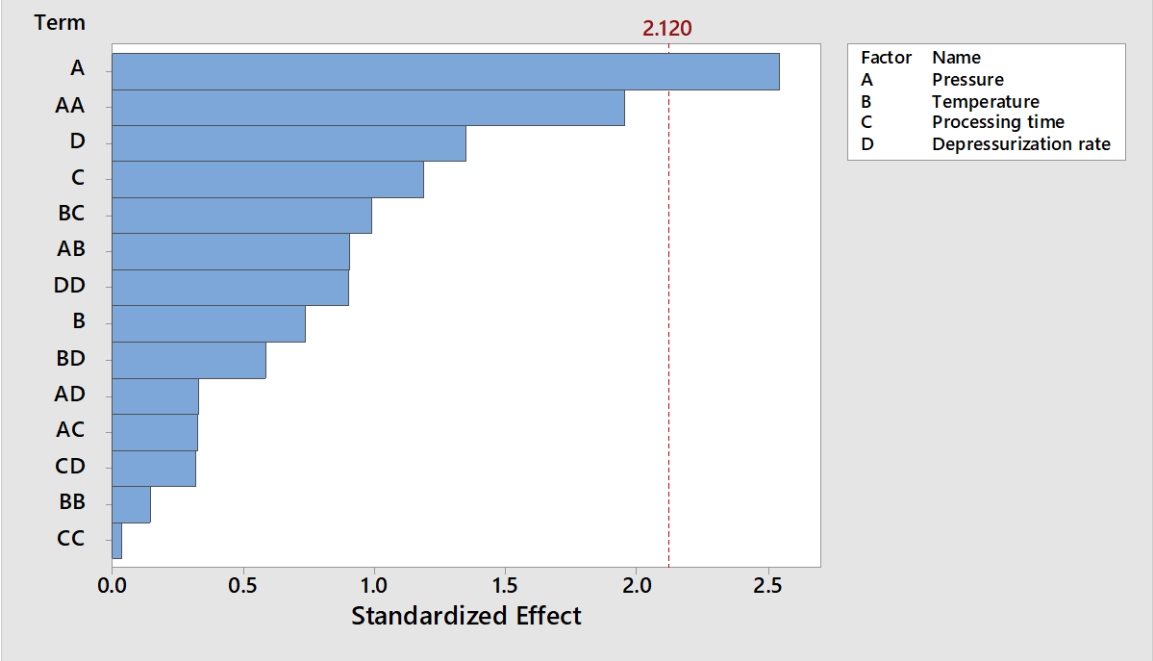

Figure 4.3. Pareto chart of the standardized effects for response *L* value (α=0.05).

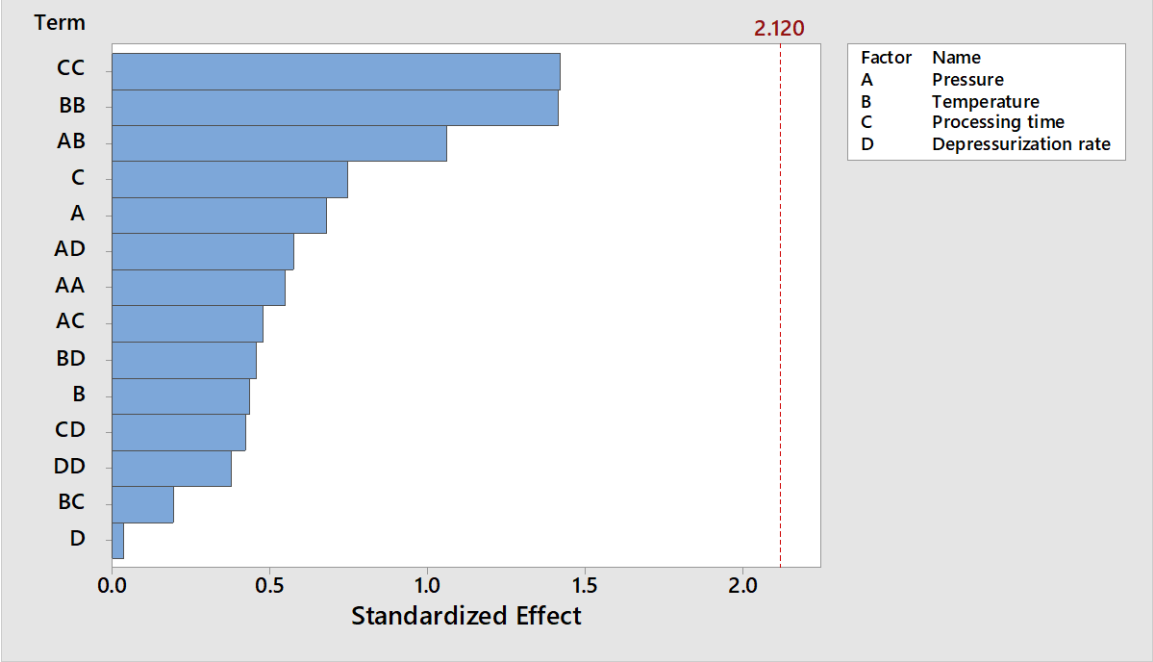

Figure 4.4. Pareto chart of the standardized effects for response *a* value (α=0.05).

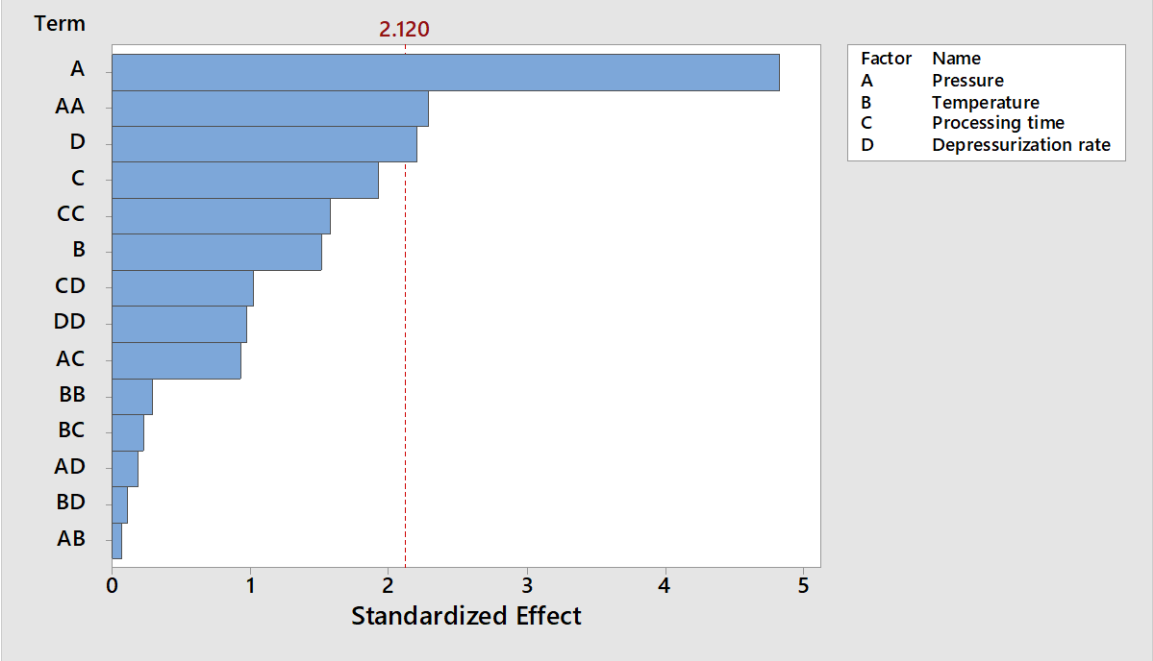

Figure 4.5. Pareto chart of the standardized effects for response *b* value (α=0.05).

The regression coefficients of the predicted simplified models for *L* and *b* are summarized in Tables 4.6 and 4.7, respectively. Proposed mathematical models are given in Eqs. (4.4) and (4.5), respectively, for *L* and *b* values.

$$\Delta Y_L = 1.56 + 0.0155\ P \tag{4.4}$$

$$\Delta Y_b = -0.62 + 0.01633\ P + 0.0138\ DR - 0.000027\ P*P \tag{4.5}$$

Table 4.6. Regression coefficients of the model for *L* value for coded coefficients.

Term	Coefficient	SE Coef.	P-Value
Constant	1.602	0.215	0
P	0.363	0.143	0.022

Table 4.7. Regression coefficients of the model for *b* value for coded coefficients.

Term	Coefficient	SE Coef.	P-Value
Constant	1.694	0.124	0
P	0.3972	0.0822	0
DR	0.1808	0.0822	0.043
*P*P*	-0.274	0.12	0.036

ANOVA results for *L* and *b* models are shown in Tables 4.8, 4.9, respectively. For the model of *L* value, the results show that the *p*-value is 0.276 and lack-of-fit error is 0.986, indicating that the fitted model is accurate enough to predict the response *L* value. For the model of *b* value, it is clear that *p*-value is 0.008, showing the model is significant at 95% confidence level. This model shows that lack-of-fit error is 0.97, indicating that the fitted model is accurate enough to predict the response *b* value.

Table 4.8. ANOVA results for *L* value model.

Source	DF	Adj SS	Adj MS	F-Value	P-Value
Model	14	7.7416	0.55297	1.36	0.276
P	1	2.6416	2.64162	6.49	0.022
Error	16	6.5149	0.40718		
Lack-of-Fit	10	1.6501	0.16501	0.2	0.986
Pure Error	6	4.8648	0.8108		
Total	30	14.2565			

Table 4.9. ANOVA results for *b* value model.

Source	DF	Adj SS	Adj MS	F-Value	P-Value
Model	14	6.82091	0.48721	3.61	0.008
P	1	3.15534	3.15534	23.35	0
DR	1	0.65393	0.65393	4.84	0.043
*P*P*	1	0.70963	0.70963	5.25	0.036
Error	16	2.16211	0.13513		
Lack-of-Fit	10	0.65568	0.06557	0.26	0.97
Pure Error	6	1.50643	0.25107		
Total	30	8.98302			

Residual plots for *L* and *b* values are shown in Figs. 4.6 and 4.7, respectively. For *L* value, Fig. 4.6 (c) shows that the data resembled normal distribution between the residual range from -1 to 1 but showing a residual at 1.5. As for the residual plot for *b* value, the results show that the majority of residuals are located in the range from -0.2 to 0.2 (Fig. 4.7 (c)). Figs. 4.6 (b, d) and 4.7 (b, d) for the two responses show that the residuals fall in a horizontal band with no systematic patterns.

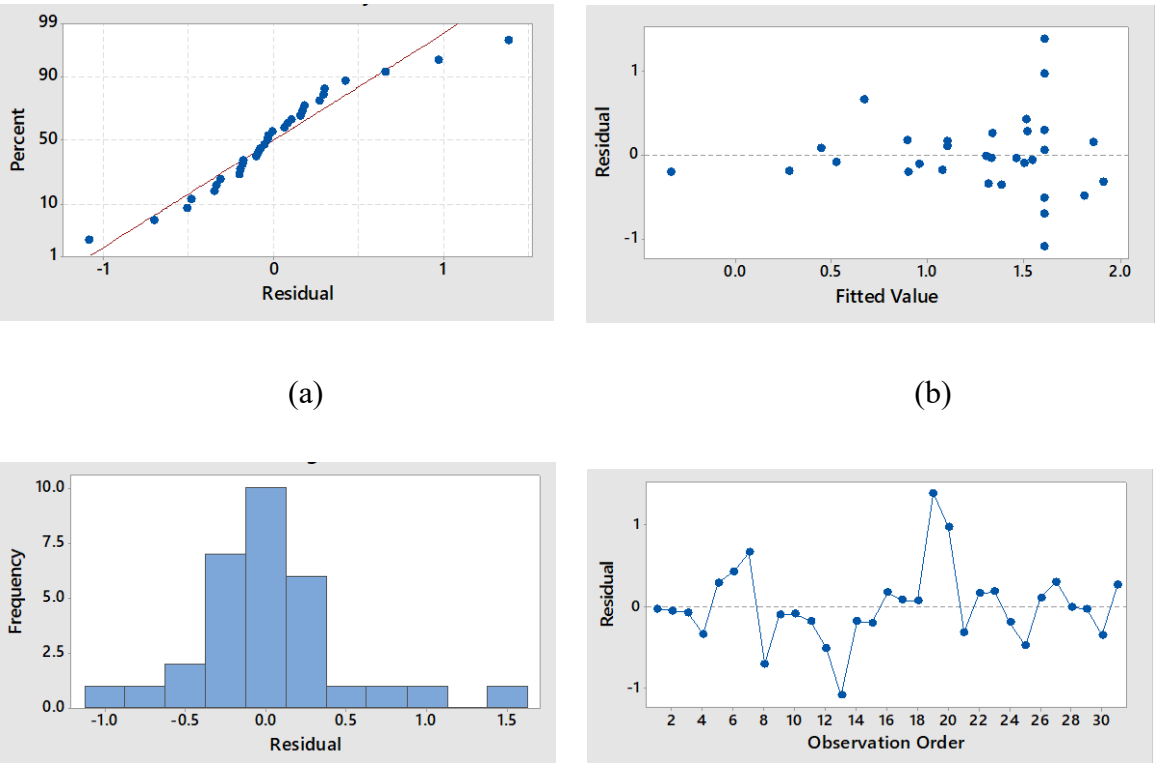

(a) (b)

(c) (d)

Figure 4.6. Residual plots for *L* value: (a) Normal probability plot for standardized residuals, (b) versus fits for standardized residuals, (c) histogram of standardized residuals, and (d) versus order for standardized residuals.

Considering the second-order model for response *b* value (Eq. (4.5)), response surfaces were generated as presented in Fig. 4.8. The surface plots for *b* value versus DR and P displayed

a convex shape. The biggest change in *b* value was observed close to *P*=250 bar and *DR*=120 bar/min condition. For *b* value, the most desirable area is in the lower left corner, which represents low *P* and *DR*.

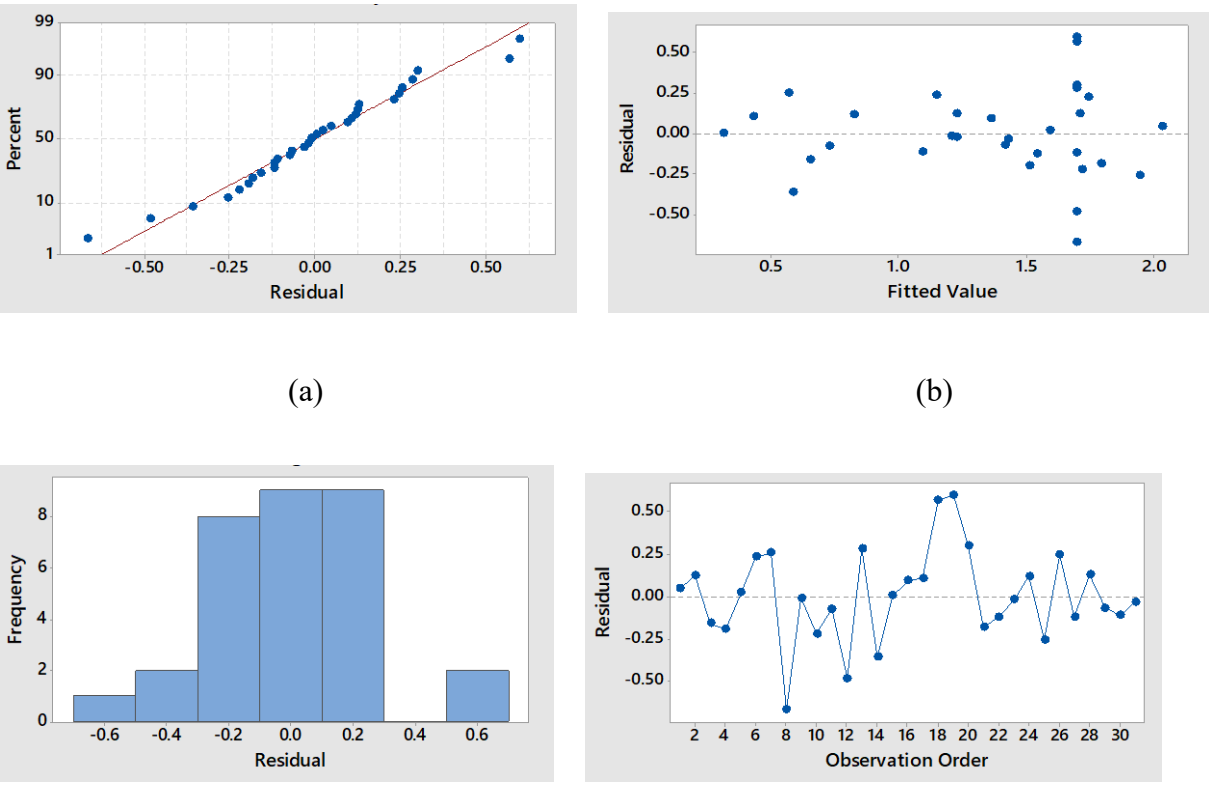

(a) (b)

(c) (d)

Figure 4.7. Residual plots for *b* value: (a) Normal probability plot for standardized residuals, (b) versus fits for standardized residuals, (c) histogram of standardized residuals, and (d) versus order for standardized residuals.

Photographs were taken during experiments to visualize how the HPCD treatment affects the color of samples. Fig. 4.9 shows some selected photographs. In all photographs, the left three

samples were treated under the various conditions specified and the right three samples were untreated. The change in appearance was substantial at the more extreme treatment conditons.

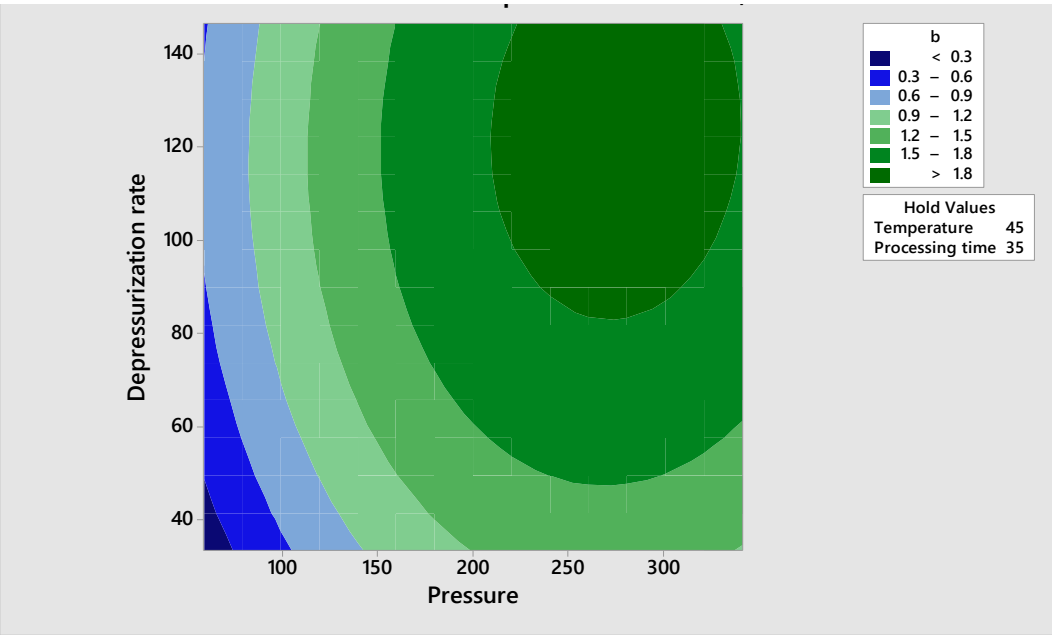

(a)

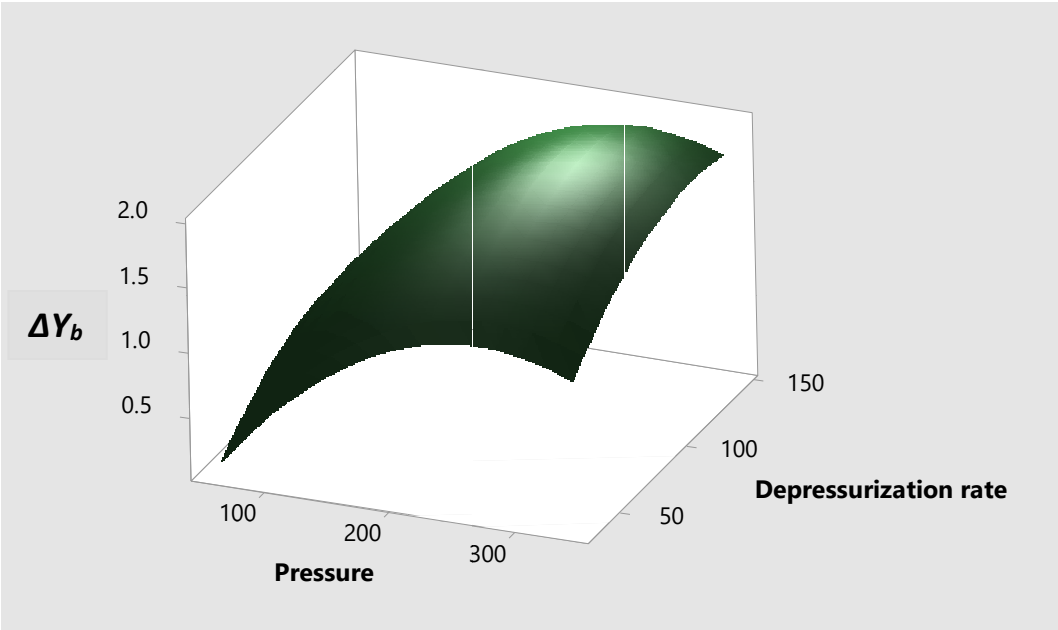

(b)

Figure 4.8. (a) Response contour and (b) surface plot (holding values: $T = 45$ ˚C, $t = 35$ min) for the effect of pressure (bar) and depressurization rate (bar/min) on b value.

200 bar, 45˚C, 63 min, 90 bar/min

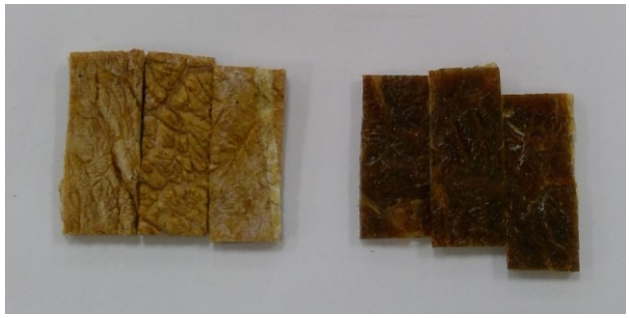

341 bar, 45˚C, 35 min, 90 bar/min

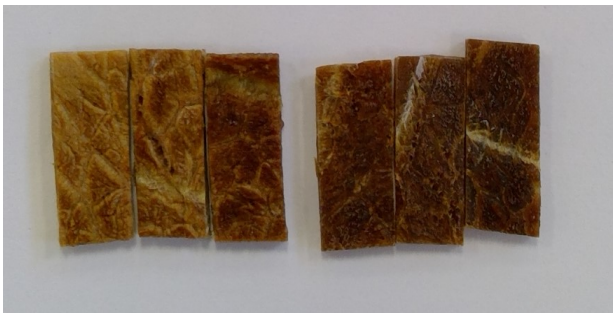

200 bar, 45˚C, 35 min, 90 bar/min

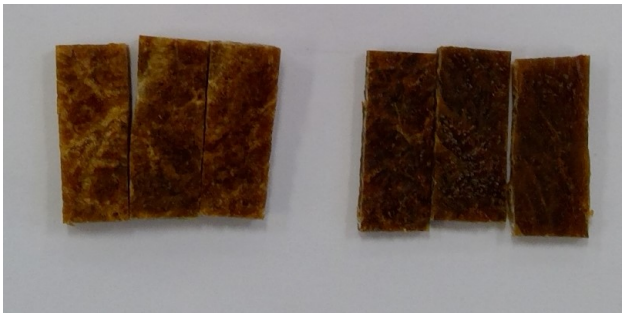

58.6 bar, 45˚C, 35 min, 90 bar/min

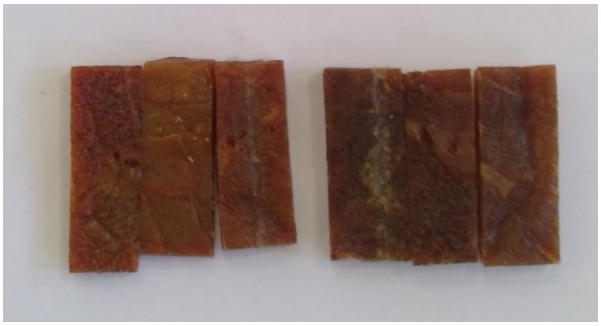

57 bar, 65˚C, 15 min, 60 bar/min

57 bar, 65˚C, 15 min, 60 bar/min (with water added)

93 bar, 59 ˚C, 36 min, 56 bar/min (optimum condition)

Figure 4.9. Photographs comparing surface color of treated and untreated beef jerky. (57 bar, 65 ˚C, 15 min, 60 bar/min is the condition reported by Schultze (2019)).

4.3.1.3 Effect on fat content

Pareto chart of fat content is shown in Fig 4.10. None of the linear, quadratic or interaction terms showed a significant effect on fat content. Therefore, further modeling was not performed.

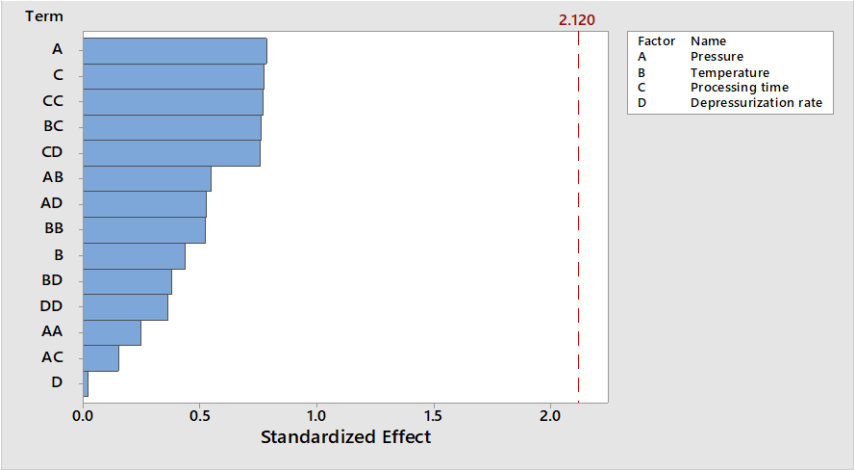

Figure 4.10. Pareto chart of the standardized effects for the response fat content (α=0.05).

4.3.1.4 Effect on WBSF

In terms of WBSF, the quadratic *DR* and linear *T* terms showed a significant (p<0.05) effect as shown in the Pareto chart (Fig. 4.11).

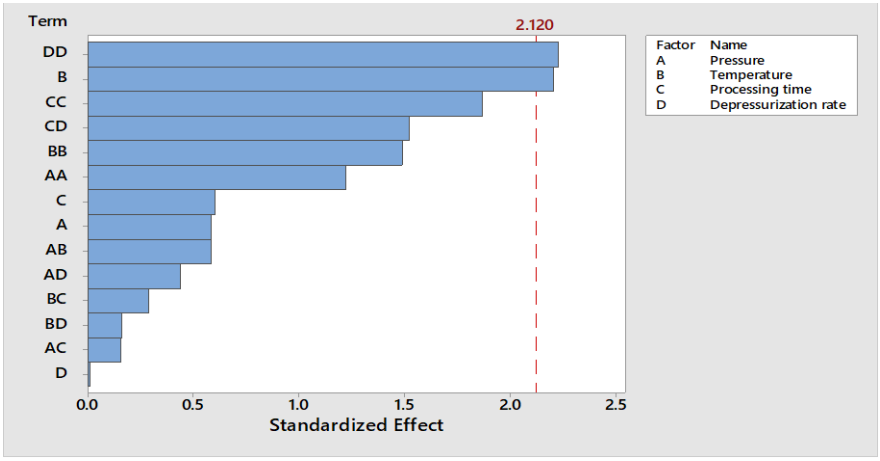

Figure 4.11. Pareto chart of the standardized effects for the response WBSF (α=0.05).

The regression coefficients of the predicted second-order polynomial model for WBSF were summarized in Table 4.10 and the proposed mathematical model is given in Eq. (4.6).

$$\Delta Y_{WBSF} = -170.6 + 4.90\ T - 0.00451\ DR*DR \quad (4.6)$$

The ANOVA results for the simplified WBSF model are shown in Table 4.11. The *p*-value of the model is 0.045, showing the model is significant at 95% confidence level. Lack-of-fit error is 0.49, indicating that the fitted model is accurate enough to predict the response of WBSF.

Table 4.10. Regression coefficients of the model for WBSF for coded coefficients.

Term	Coefficient	SE Coef.	P-Value
Constant	12.12	3.35	0.002
T	4.9	2.22	0.042
*DR*DR*	-7.21	3.24	0.04

Table 4.11. ANOVA results for WBSF.

Source	DF	Adj SS	Adj MS	F-Value	P-Value
Model	14	3368.89	240.635	2.44	0.045
T	1	479.91	479.907	4.86	0.042
*DR*DR*	1	490.76	490.764	4.97	0.04
Error	16	1579.07	98.692		
Lack-of-Fit	10	1010.75	101.075	1.07	0.49
Pure Error	6	568.32	94.72		
Total	30	4947.96			

Residual plots for WBSF are shown in Fig 4.12. Fig. 4.12 (c) shows that the data somewhat resembled normal distribution. Figs. 4.12 (b, d) show that the residuals fall in a horizontal band with no systematic pattern.

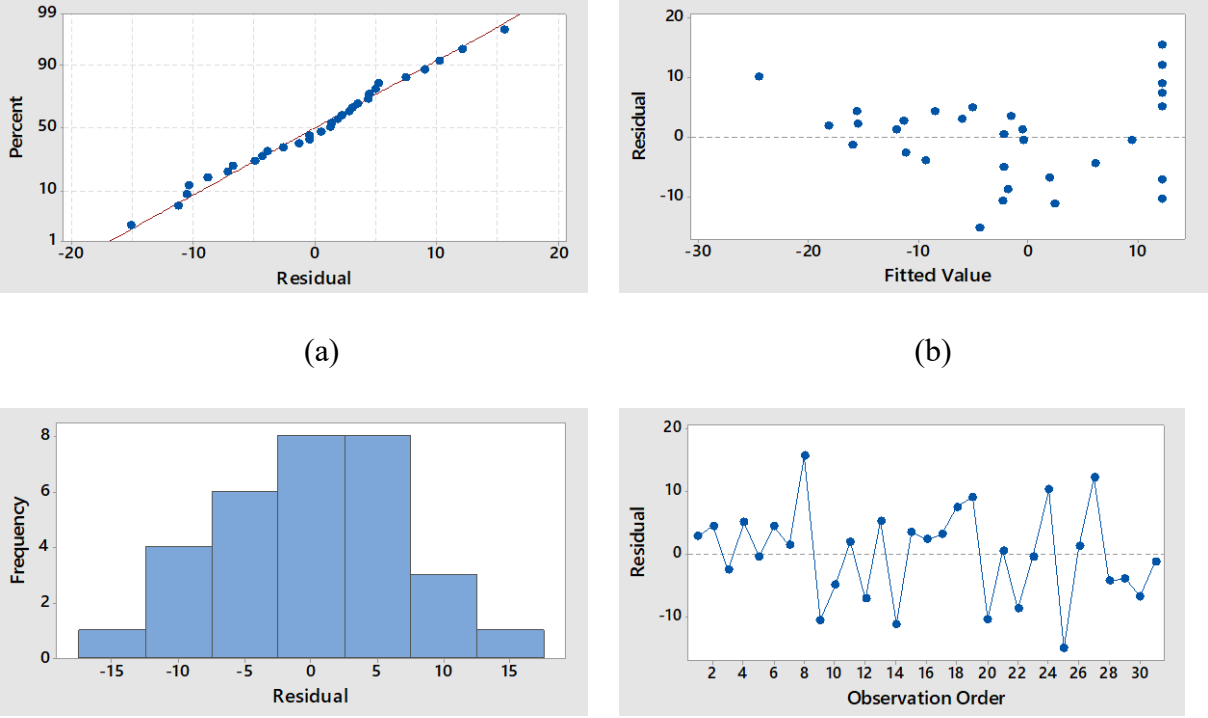

Figure 4.12. Residual plots for WBSF: (a) Normal probability plot for standardized residuals, (b) versus fits for standardized residuals, (c) histogram of standardized residuals, and (d) versus order for standardized residuals.

Response contour and surface plots for WBSF are presented in Fig. 4.13. As shown in the surface plot, ΔY_{WBSF} increased the most in the center circle area. Contour plot shows that the desirable area of WBSF is located on the junction line between the first and second light green areas. Inside the junction circle line between the first and second light green areas, ΔY_{WBSF} is positive, indicating that there is an increase in the WBSF. Outside the junction line, ΔY_{WBSF} is negative, which represents a decrease in the WBSF.

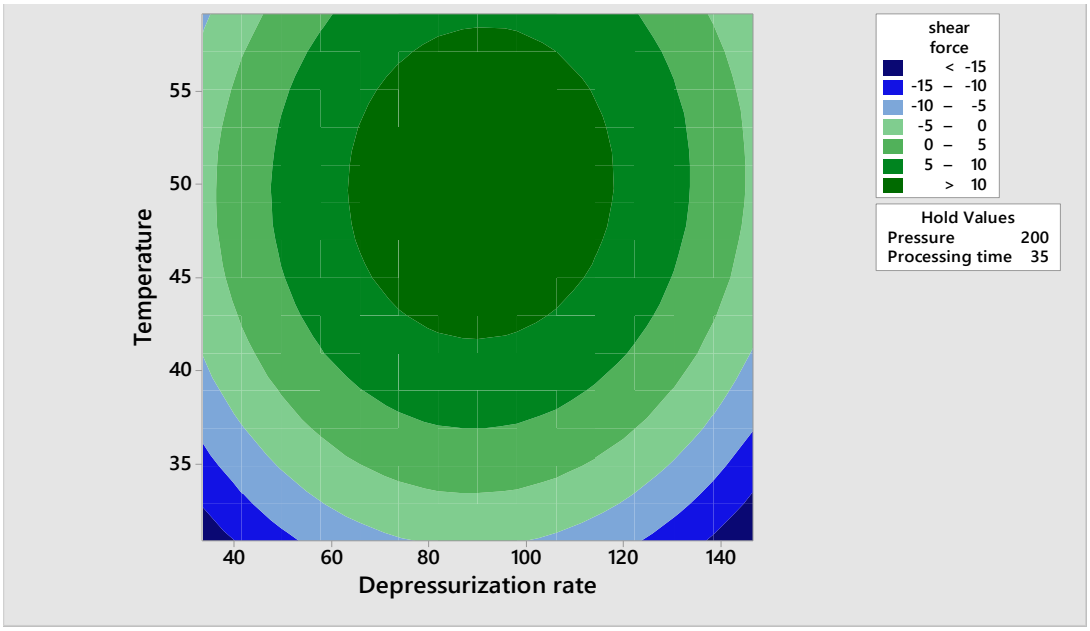

(a)

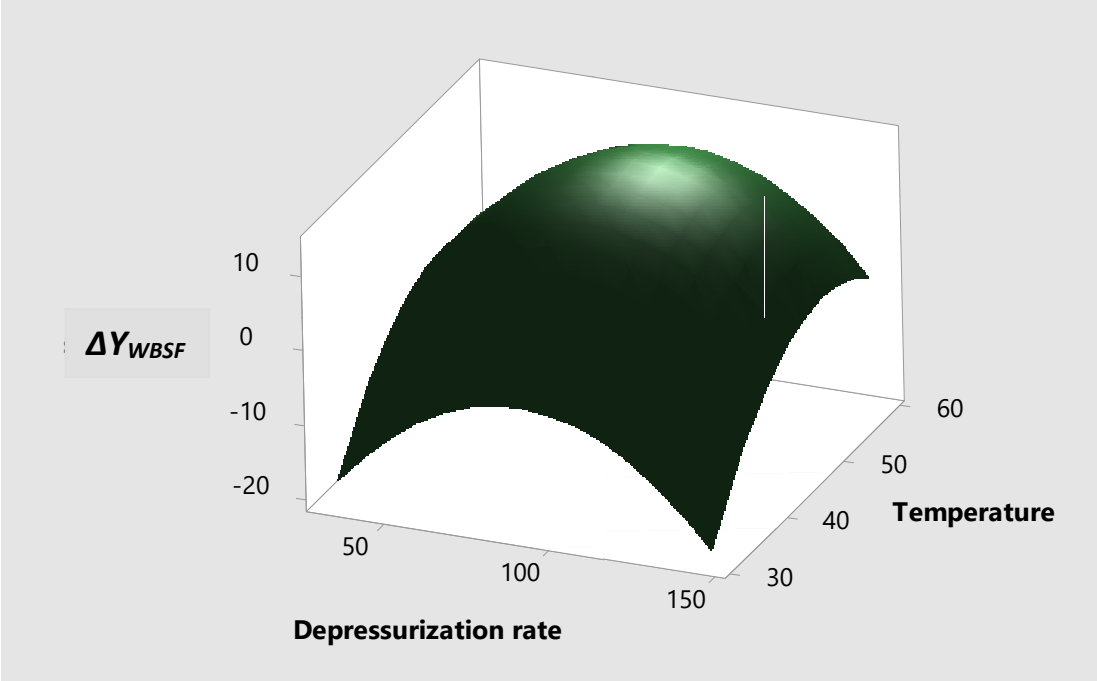

(b)

Figure 4.13. (a) Response contour and (b) surface plots (hold values: P = 200 bar, t = 35 min) for the effects of depressurization rate (bar/min) and temperature (˚C) on WBSF.

4.3.2 Optimization of HPCD treatment conditions

The desirability function technique was used for the parameter optimization. According to this function, the measured quality characteristics of every predicted response is transformed to a dimensionless desirability (d) value ranging between d=0 and d=1. The value of d increases as the desirability of the corresponding response increases. In this study, four responses were set at d=1 equally. To make the color profile weight equal to 1, *L*, *a* and *b* value responses were all set at d=0.33 with an equal weight among the three color parameters. Table 4.12 shows the optimum condition obtained using the Minitab software.

Table 4.12. Optimum HPCD condition generated by Minitab software.

***P*(bar)**	***T*(˚C)**	***t*(min)**	***DR*(bar/min)**
92.88	59.14	35.86	56.3

Table 4.13 shows the comparison between the experimental results and predicted values under the optimum condition, which were in agreement. Table 4.14 shows the comparison of experimental results and predicted values under the condition: *P*=57 bar, *T*=65˚C, *t*=15 min, *DR*=60 bar/min with the addition of water, which was established by Schultze (2019) to maximize microbial inactivation.

Table 4.13. Comparison between experimental and predicted results under the optimum condition: *P*=93 bar, *T*=59 ˚C, *t*=36 min, *DR*=56 bar/min.

Response	Experimental result (Δ*Y*)	Predicted value	*Y'*
a_w	-0.018	-0.021	0.77
L	0.008	0.007	79.74
a	0.260	0.384	2.09
b	0.220	0.659	-0.85
Fat content	-0.011	-0.013	3.69%
WBSF	-6.62	-1.11	32.04 N

Table 4.14. Comparison between experimental and predicted results under the condition: *P*=57 bar, *T*=65˚C, *t*=15 min, *DR*=60 bar/min with the addition of water, established by Schultze (2019).

Response	Experimental result (Δ*Y*)	Predicted value	*Y'*
a_w	-0.0145	-0.010	0.78
L	0.794	-1.287	84.68
a	0.268	0.171	2.47
b	0.090	-0.132	-1.02
Fat content	-0.022	-0.020	2.65%
WBSF	5.649	-11.718	39.10 N

4.3.3 Morphology analysis

As shown in Fig. 4.14, untreated and treated under the optimum condition samples showed similar morphologies of compact muscle fibres. Fig. 4.14 (c) shows that the sample treated under *P*=57 bar, *T*=65˚C, *t*=15 min, *DR*=60 bar/min condition, which was the best condition in terms of microbial inactivation (Schultze, 2019), showed larger spaces between muscle fibre tissues. Fig. 4.14 (d) demonstrates that adding water under the same condition could minimize the effect and shows moderate space between muscle fibres.

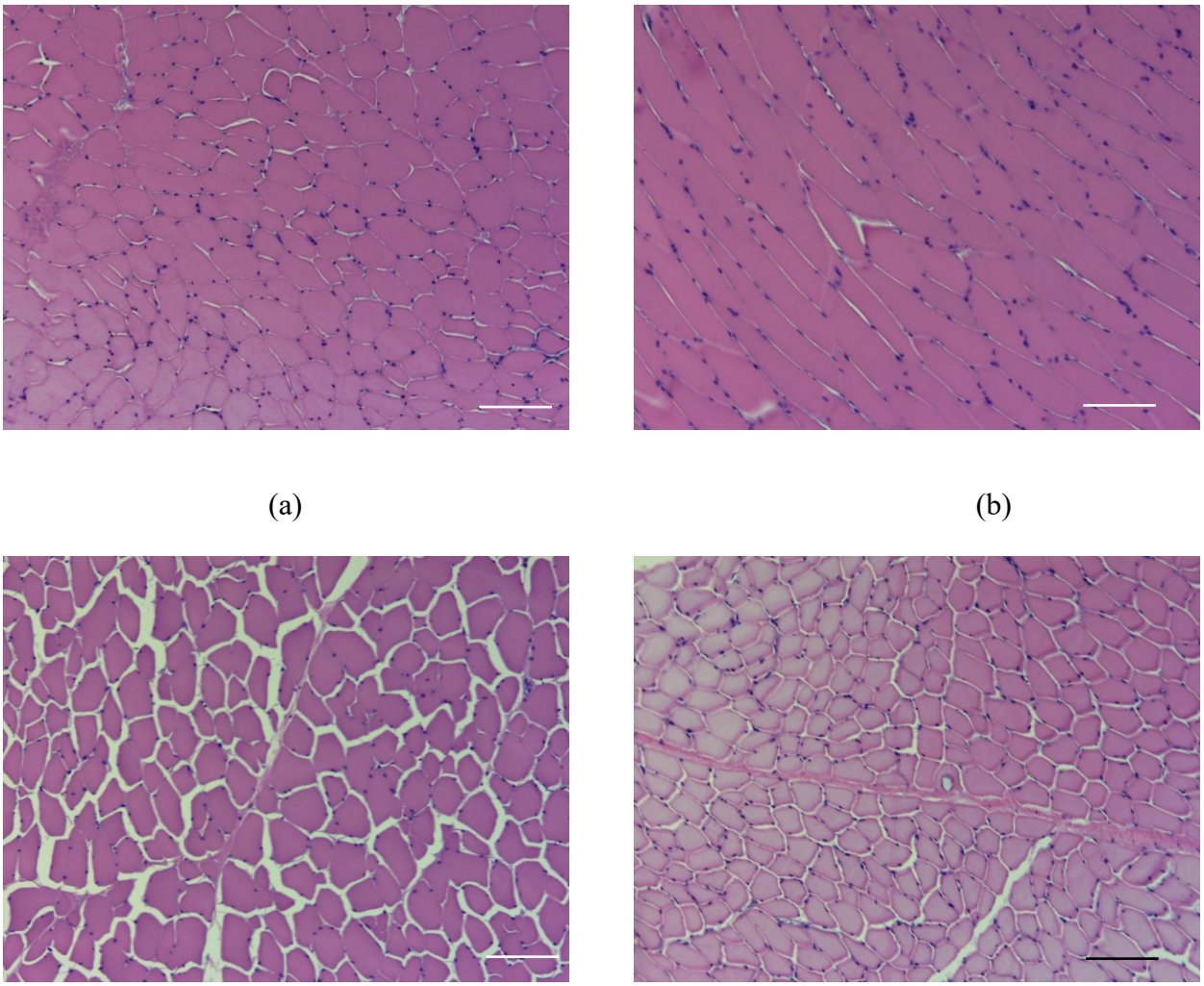

(a) (b)

(c) (d)

Figure 4.14. Light microscopy images (scale bars represent 100 µm) for (a) untreated sample; (b) treated under the optimum condition: *P*=93 bar, *T*=59 ˚C, *t*=36 min, *DR*=56 bar/min; (c) treated under: *P*=57 bar, *T*=65˚C, *t*=15 min, *DR*=60 bar/min (Schultze, 2019); (d) treated under: *P*=57 bar, *T*=65˚C, *t*=15 min, *DR*=60 bar/min with the addition of water (Schultze, 2019).

4.4 Discussion

The a_w of beef jerky samples decreased after the HPCD treatment at different conditions. Since the CO_2 used during processing was dry CO_2 (< 3 ppm H_20), free water in the sample would solubilize into the CO_2 phase, in an effort to reach equilibrium of water. According to

Wang, Zhou, Guo, Yang and Lu (2018), the water solubility (the mole fraction of H_2O in the homogeneous supercritical CO_2 phase, x_{H2O}) in supercritical CO_2 is 0.0093 and 0.0129 at 40 and 60 ˚C at 200 bar, respectively. Wang et al. (2018) demonstrated that the solubility of water in HPCD increases exponentially with increasing temperature at constant pressure. In addition, available free water content in beef jerky also increases with temperature, as was reported in Chapter 3 (section 3.3.4). As a result of both reasons, increasing *T* would accelerate free water moving into the CO_2 phase, and therefore *T* showed a significant influence on a_w reduction (Lewicki, 2004).

There was an increase in *L* and *b* values of beef jerky samples to different extents, depending on the conditions applied. Cappelletti, Ferrentino and Spilimbergo (2015) found higher *L* and *b* values but a lower *a* value for raw pork meat treated with HPCD. Choi et al. (2013) also reported a higher *L* value, lower *a* value and no significant change in *b* value after HPCD treatment. According to Choi et al. (2013), one of the pork products marinated with soy sauce that was treated at 152 bar, 31.1˚C for 10 min showed a significantly paler surface color than the control. In the present study, a similar result was found for beef jerky samples treated under different conditions, i.e. 200 bar, 45˚C, 63 min, 90 bar/min (Fig. 4.9) An increasing *L* value after HPCD treatment is the result of the changes in proteins. After HPCD treatment, an increase in denatured proteins was detected, especially the sarcoplasmic proteins in fresh pork meat (Choi et al., 2008). The changes in *L* and *a*, and paler surface color are believed to be related to the denaturation of sarcoplasmic proteins (phosphorylase b, creatine kinase, triosephophate isomerase and one unknown protein) in meat (Choi et al., 2008). It is worth to mention that meat samples treated with high hydrostatic pressure (HHP) treatment also showed an increase in *L* value (Campus, Flores, Martinez and Toldra, 2008; Yi et al., 2013). HHP

treatment leads to coagulation of the protein, increasing light reflection and creating a whitened color. It is well known that myoglobin and its oxidative state are responsible for the red color of meat. Cava, Ladero, Gonzalez, Carrasco and Ramirez (2009) reported that discoloration of meat with HPP treatment was caused by the oxidation of ferrous myoglobin to ferric myoglobin. Moller and Skibsted (2006) reported that globin denaturation, heme displacement or release may also result in meat discoloration through the HHP process. It is possible that similar changes can occur during the HPCD treatment; however, the literature lacks such information. On the other hand, the HHP process changes the structure (mainly depolymerization) of the protein, which creates an increase in the ratio of the light reflected and absorbed by the material (Rodrigues et al., 2016). In terms of the *a* value, HHP treatment is believed to lead to a lower *a* value when $P >$ 3000 bar, and there was no significant change or even a slight increase when $P <$ 3000 bar (Carles, Veciana-Nogues, and Cheftel, 1995). Apparently, the pressure levels used in this study were substantially lower than 3000 bar, but regardless there was a change in the *L* and *b* values.

The change in the fat content of the majority of the samples was small, and none of the input variables had a significant effect on the reduction of fat content. This is due to the fact that the studied processing conditions were too mild to show a difference. Rahman, Seo, Choi, Gul, and Yang (2018) extracted bovine heart (~15.42% fat) using a CO_2 flow rate of 30-50 g/min at 400 bar and 40˚C for 5 h to get a defatted bovine heart (~1% fat). Based on the equation generated by Güçlü-Üstündağ and Temelli (2000), the solubility of triolein in HPCD phase is 0.9675 g/L at 50 ˚C and 200 bar. The low solubility of triglycerides in HPCD under the conditions tested contributes to the small change in the fat content of the beef jerky in this study.

In terms of texture, beef jerky was either tenderized or toughened after the HPCD treatment under different conditions. Firstly, *T* showed a significant effect on WBSF instead of *P*.

According to Rastogi, Raghavarao, Balasubramaniam, Niranjan, and Knorr (2007), pressure-induced denaturation of proteins is normally reversible when P < 3000 bar. Therefore, *P* does not have a significant effect on the texture of meat. Different from high *P,* increased *T* can cause destruction of hydrogen and covalent bonds, which leads to the variation in meat texture (Sun and Holley, 2010). The tenderizing effect of HHP treatment on meat products is because HHP results in structural changes in the myofibrils (Cheftel and Culioli, 1997; Suzuki, Kim, Homma, Ikeuchi, and Saito, 1992). The toughening effect could be associated with muscle fibre elongation induced by HHP treatment (Vaudagna et al., 2012). In terms of HPCD treatment, a higher tenderness of ground beef and marinated pork was reported after HPCD treatment (Meurehg, 2006; Choi et al., 2013).

4.5 Conclusions

In this study, response surface methodology (RSM) was employed to model the effects of HPCD treatment on the physicochemical properties of beef jerky as a function of temperature, pressure, time and depressurization rate. *T* showed a significant effect on a_w; *P*, P^2 and *DR* exerted a significant effect on surface color; no input variable had a significant effect on fat content, while DR^2 and *T* showed a significant effect on WBSF of beef jerky sample after HPCD treatment. An optimum HPCD treatment condition was determined via RSM model to minimize the changes in responses, which was *P*=92.9 bar, *T*=59.1˚C*, t*=35.9 min and *DR*=56.3 bar/min. Such a treatment shows potential for the use of HPCD treatment to enhance the safety of beef jerky products while minimizing changes in its quality attributes.

Chapter 5: Conclusions and Recommendations

5.1 Summary of key findings

In this thesis research, the influence of high-pressure carbon dioxide (HPCD) treatment on the moisture sorption isotherm and physicochemical properties of beef jerky was studied in an effort to contribute to further development of HPCD treatment to enhance the safety and quality of low water activity (a_w) food products. Compared to either air or CO_2 environment at ambient pressure, the shape of the moisture sorption isotherm under HPCD environment changed from type II to type III, which was demonstrated for the first time (Chapter 3). With increasing pressure of the CO_2 environment from 57 and 200 bar, the isotherms became very steep at a_w level of 0.73 and 0.70, respectively. This behavior was attributed to the effect of HPCD treatment on the interactions between protein, salt and water present in the beef jerky. In addition, the net isosteric heat of sorption of water was found to be higher in the low moisture content range in the CO_2 environment compared to the air environment, which indicated that more energy was needed to vaporise water from the food matrix. Therefore, CO_2 performed like a "glue" between water molecules and food matrix, making water less available in the CO_2 environment at low moisture content range. Because water plays an important role (i.e. formation of carbonic acid) for microbial inactivation by HPCD, it is more challenging to inactivate microorganisms in low a_w foods by HPCD. The findings contribute to better understanding of the changes in HPCD environment and the microbial inactivation mechanisms in low a_w products so that new strategies can be developed to enhance the efficacy of the HPCD treatment.

In terms of the physicochemical properties, response surface methodology was used to investigate the effects of HPCD treatment parameters (pressure, temperature, processing time,

and depressurization rate) on the a_w, color profile (L, a, b), fat content, and Warner-Bratzler shear force of beef jerky (Chapter 4). The results demonstrated that pressure, temperature and depressurization rate had significant influence on the response variables evaluated. Specifically, a_w was affected by temperature, surface color was influenced by pressure, quadratic pressure and depressurization rate; no input variable had a significant effect on fat content, and Warner-Bratzler shear force was affected by quadratic depressurization rate and temperature. Within the range of levels investigated, the optimum HPCD treatment condition to minimize the changes in the physicochemical properties was determined as P=92.9 bar, T=59.1˚C, t=35.9 min and DR=56.3 bar/min.

This thesis research was part of a larger project, focusing on the HPCD treatment as a technique to enhance the microbial safety of low water activity food products while minimizing quality changes. Based on the findings of this thesis research, HPCD treatment shows potential to be a processing aid for beef jerky products while minimizing changes in its quality attributes.

5.2 Recommendations for future work

Despite the great potential demonstrated, there are remaining questions that need to be answered and more research is needed before HPCD can be used in large scale food industries.

In future studies, other analysis techniques can be applied for better understanding of the phenomenon at the molecular level. For instance, the use of pulsed nuclear magnetic resonance to probe water relations in foods is a feasible approach to study water molecular mobility in food systems. The challenge is to apply such techniques under high pressure CO_2 environment to demonstrate the impact of CO_2 on the interactions of water with other food components as well as microorganisms. In this research, attempts were made to measure the relative humidity *in situ*

under high pressure CO_2 condition, unfortunately, the sensor was not operational when placed in a 100% CO_2 environment. Therefore, the samples have to be removed from the high pressure chamber for a_w and moisture content determinations; however, water solubilized into the supercritical CO_2 phase precipitates back on the sample during depressurization, Since there is no available device currently to determine the relative humidity under high pressure CO_2 condition, it is worthwhile to develop a theoretical model and new sensor to measure relative humidity under HPCD condition. Such approaches will contribute to unraveling the microbial inactivation mechanisms under low moisture conditions. The microbial inactivation efficiency under the optimum condition generated in the present study needs to be determined.

Regarding the quality aspects, it would be valuable to investigate the effect of HPCD saturated with water on the quality parameters of beef jerky since water-saturated HPCD showed a higher inactivation efficiency in a parallel study by Schultze (2019). In addition, it is worthwhile to investigate in the future, the effects of HPCD treatment on the sensory properties of beef jerky to relate the physicochemical properties evaluated in this study by instrumental techniques to sensory attributes. Potential changes in flavor were not assessed and this needs to be evaluated using a sensory panel since flavor is the top priority attribute for customers to choose a food product. Beef jerky is just one example out of a large number of low water activity foods. Therefore, more research could be conducted on other low moisture foods, for example, nuts, flour, and dry fruit with similar approaches to assess the impact of HPCD treatment on their quality attributes.

Bibliography

Aavatsmark, I., & Kaufmann, R. (2015). A simple function for the solubility of water in dense-phase carbon dioxide. International Journal of Greenhouse Gas Control, 32, 47-55.

Ahmad, M., Gersen, S., & Wilbers, E. (2014). Solubility of water in CO_2 mixtures at pipeline operation conditions. International Journal of Chemical, Materials Science and Engineering, 8(4), 1-6. A

Al-Mahasneh, M., Alkoaik, F., Khalil, A., Fulleros, R., & El-Waziry, A. (2014). Effect of temperature on moisture sorption isotherms and monolayer moisture content of Bermuda grass (*Cynodon dactylon*). Bulgarian Journal of Agricultural Science, 20(6), 1289-1294.

Al-Muhtaseb, A. H., McMinn, W. A. M., & Magee, T. R. A. (2002). Moisture sorption isotherm characteristics of food products: a review. Food and Bioproducts Processing, 80(2), 118-128.

Anderson, R. B. (1946). Modifications of the Brunauer, Emmett and Teller equation. Journal of the American Chemical Society, 68(4), 686-691.

AOAC. (1984). Official Methods of Analysis of the Association of Official Analytical Chemists, 14th ed. Washington. DC.

Aviles B., Klotz C., Smith T., Williams R., Ponder M. 2013. Survival of *Salmonella enterica* serotype Tennessee during simulated gastric passage is improved by low water activity and high fat content. Journal of Food Protection. 76: 333-337.

Azuara, E., & Beristain, C. I. (2006). Enthalpic and entropic mechanisms related to water sorption of yogurt. Drying Technology, 24(11), 1501-1507.

Bamberger, A., Sieder, G., & Maurer, G. (2004). High-pressure phase equilibrium of the ternary system carbon dioxide+ water+ acetic acid at temperatures from 313 to 353 K. The Journal of Supercritical Fluids, 32(1-3), 15-25.

Bando, S., Takemura, F., Nishio, M., Hihara, E., & Akai, M. (2003). Solubility of CO_2 in aqueous solutions of NaCl at (30 to 60) C and (10 to 20) MPa. Journal of Chemical & Engineering Data, 48(3), 576-579.

Basu, S., Shivhare, U. S. and Mujumdar, A. S. (2006). Models for sorption isotherms for foods: a review. Drying Technology. 24: 917-930.

Bell, L. N., & Labuza, T. P. (2000). Practical aspects of moisture sorption isotherm measurement and use. 2nd. ed., AACC Eagan Press, Eagan, MN.

Berlin, E. (1978). Hydration on milk proteins. Water activity: Influences on food quality: a treatise on the influence of bound and free water on the quality and stability of foods and other natural products (USA). Academic Press.

Booth, I. R. (1985). Regulation of cytoplasmic pH in bacteria. Microbiological Reviews, 49(4), 359.

Borowski, A. G., Ingham, S. C., & Ingham, B. H. (2009). Validation of ground-and-formed beef jerky processes using commercial lactic acid bacteria starter cultures as pathogen surrogates. Journal of Food Protection, 72(6), 1234-1247.

Bowman, L. E., Palmer, B. J., Garrett, B. C., Fulton, J. L., Yonker, C. R., Pfund, D. M., & Wallen, S. L. (1996). Infrared and molecular dynamics study of D_2O rotational relaxation in supercritical CO_2 and Xe. The Journal of Physical Chemistry, 100(47), 18327-18334.

Brown, W. D., and Mebine, L. B. (1969). Autoxidation of oxymyoglobins. Journal of Biological Chemistry, 244, 6696-6701.

Bruin, S., & Luyben, K. C. A. (1980). Recent developments in dehydration of food materials. Food Process Engineering, 1, 466-822.

Brunauer, S., Deming, L. S., Deming, W. E., & Teller, E. (1940). On a theory of the van der Waals adsorption of gases. Journal of the American Chemical society, 62(7), 1723-1732.

Brunauer, S., Emmett, P. H., & Teller, E. (1938). Adsorption of gases in multimolecular layers. Journal of the American Chemical Society, 60(2), 309-319.

Buckee, G. K. (1994). Determination of total nitrogen in barley, malt and beer by Kjeldahl procedures and the Duma combustion method collaborative trial. Journal of the Institute of Brewing, 100(2), 57-64.

Calvo, M. M., & Balcones, E. (2001). Inactivation of microorganisms and changes of proteins during treatment of milk with subcritical carbon dioxide. Milchwissenschaft, 56(7), 366-369.

Campus,M., Flores,M., Martinez, A., & Toldra, F. (2008). Effect of high pressure treatment on colour, microbial and chemical characteristics of dry cured loin. Meat Science, 80(4), 1174–1181.

Cappelletti, M., Ferrentino, G., & Spilimbergo, S. (2015). High pressure carbon dioxide on pork raw meat: Inactivation of mesophilic bacteria and effects on colour properties. Journal of Food Engineering, 156, 55-58.

Carlez, A., Veciana-Nogues, T., & Cheftel, J. C. (1995). Changes in colour and myoglobin of minced beef meat due to high pressure processing. LWT-Food Science and Technology, 28(5), 528-538.

Cava, R., Ladero, L., González, S., Carrasco, A., & Ramírez, M. R. (2009). Effect of pressure and holding time on colour, protein and lipid oxidation of sliced dry-cured Iberian ham and loin during refrigerated storage. Innovative Food Science & Emerging Technologies, 10(1), 76-81.

Cheftel, J. C., & Culioli, J. (1997). Effects of high pressure on meat: a review. Meat Science, 46(3), 211-236.

Chen, C. S., & Clayton, J. T. (1971). The effect of temperature on sorption isotherms of biological materials. Transactions of the ASAE, 14(5), 927-0929.

Chinachoti, P., & Steinberg, M. P. (1984). Interaction of sucrose with starch during dehydration as shown by water sorption. Journal of Food Science, 49(6), 1604-1608.

Chirife, J., & Iglesias, H. A. (1978). Equations for fitting water sorption isotherms of foods: Part 1—a review. International Journal of Food Science & Technology, 13(3), 159-174.

Choi, Y. M., Lee, S. H., Choe, J. H., Kim, K. H., Rhee, M. S., & Kim, B. C. (2013). Effects of supercritical carbon dioxide treatment on meat quality and sensory evaluation in soy sauce and hot-pepper paste marinated pork. Korean Journal for Food Science of Animal Resources, 33(5), 581-586.

Choi, Y. M., Ryu, Y. C., Lee, S. H., Go, G. W., Shin, H. G., Kim, K. H., ... & Kim, B. C. (2008). Effects of supercritical carbon dioxide treatment for sterilization purpose on meat quality of porcine longissimus dorsi muscle. LWT-Food Science and Technology, 41(2), 317-322.

Chrastil, J. (1982). Solubility of solids and liquids in supercritical gases. The Journal of Physical Chemistry, 86(15), 3016-3021.

Clarke, M. J., Harrison, K. L., Johnston, K. P., & Howdle, S. M. (1997). Water in supercritical carbon dioxide microemulsions: spectroscopic investigation of a new environment for aqueous inorganic chemistry. Journal of the American Chemical Society, 119(27), 6399-6406.

Comak, G., Foltran, S., Ke, J., Perez, E., Sanchez-Vicente, Y., George, M. W., & Poliakoff, M. (2016). A synthetic-dynamic method for water solubility measurements in high pressure CO_2 using ATR–FTIR spectroscopy. The Journal of Chemical Thermodynamics, 93, 386-391.

Comaposada, J., Gou, P., Pakowski, Z., & Arnau, J. (2000). Desorption isotherms for pork meat at different NaCl contents and temperatures. Drying Technology, 18(3), 723-746.

Condon, J. B. (2006). Surface area and porosity determinations by physisorption: measurements and theory. Elsevier, Amsterdam. The Netherlands.

Damar, S., & Balaban, M. O. (2006). Review of dense phase CO_2 technology: microbial and enzyme inactivation, and effects on food quality. Journal of Food Science, 71(1), R1-R11.

de Boer, J. H. (1953). The Dynamical Character of Adsorption. Clarendon Press.

Debs-Louka, E., Louka, N., Abraham, G., Chabot, V., & Allaf, K. (1999). Effect of compressed carbon dioxide on microbial cell viability. Applied Environmental Microbiology, 65(2), 626-631.

Decker, E. A., & Park, Y. (2010). Healthier meat products as functional foods. Meat Science, 86(1), 49-55.

Delgado, A. E., & Sun, D. W. (2002). Desorption isotherms for cooked and cured beef and pork. Journal of Food Engineering, 51(2), 163-170.

Dillow, A. K., Dehghani, F., Hrkack, J. S., Foster, N. R., Langer, R. (1999). Bacterial inactivation by using near- and supercritical carbon dioxide. Proceedings of the National Academy of Science of the United States of America, 96, 10333-10348.

Dixon, N. M., & Kell, D. B. (1989). The inhibition by CO_2 of the growth and metabolism of micro‐ organisms. Journal of Applied Bacteriology, 67(2), 109-136.

Duan, Z., & Sun, R. (2003). An improved model calculating CO_2 solubility in pure water and aqueous NaCl solutions from 273 to 533 K and from 0 to 2000 bar. Chemical Geology*, 193(*3-4), 257-271.

Eklund, T. (1984). The effect of carbon dioxide on bacterial growth and on uptake processes in bacterial membrane vesicles. International Journal of Food Microbiology, 1(4), 179-185.

Enomoto, A., Nakamura, K., Nagai, K., Hashimoto, T., & Hakoda, M. (1997). Inactivation of food microorganisms by high-pressure carbon dioxide treatment with or without explosive decompression. Bioscience, Biotechnology, and Biochemistry, 61(7), 1133-1137.

Erkmen, O. (2000). Antimicrobial effect of pressurised carbon dioxide on *Enterococcus faecalis* in physicological saline and foods. Journal of the Science of Food and Agriculture, 80(4), 465-470.

FAO, WHO. 2015. Code of hygienic practice for low-moisture Foods, Codex Aliment. Int. Stand.

Ferrentino, G., & Spilimbergo, S. (2011). High pressure carbon dioxide pasteurization of solid foods: current knowledge and future outlooks. Trends in Food Science & Technology, 22(8), 427-441.

Ferrentino, G., Calix, T., Poletto, M., Ferrari, G., Balaban, M.O., 2012. Experimental measurement of carbon dioxide solubility. In: Balaban, M.O., Ferrentino, G. (Eds.), Dense Phase Carbon Dioxide: Food and Pharmaceutical Applications. Blackwell Publishing, p. 43.

Ferrini, G., Comaposada, J., Arnau, J., & Gou, P. (2012). Colour modification in a cured meat model dried by Quick-Dry-Slice process® and high pressure processed as a function of NaCl, KCl, K-lactate and water contents. Innovative Food Science & Emerging Technologies, 13, 69-74.

Gangola, P., & Rosen, B. P. (1987). Maintenance of intracellular calcium in *Escherichia coli.* Journal of Biological Chemistry, 262(26), 12570-12574.

Garcia-Gonzalez, L., Geeraerd, A. H., Spilimbergo, S., Elst, K., Van Ginneken, L., Debevere, Van Impe, J.F., & Devlieghere, F. (2007). High pressure carbon dioxide inactivation of microorganisms in foods: the past, the present and the future. International Journal of Food Microbiology, 117(1), 1-28.

Gibson, R. E. (1938). On the effect of pressure on the solubility of solids in liquids. American Journal of Science, 35, 49-69.

Glasstone, S., and Lewis, D. (1960). Elements of Physical Chemistry, pp. 251-253. Princeton, NJ: Van Nostrand Co., Inc.

Greenspan, L. (1977). Humidity fixed points of binary saturated aqueous solutions. Journal of Research of the National Bureau of Standards, 81(1), 89-96.

Gregg, S. J., Sing, K. S. W., & Salzberg, H. W. (1967). Adsorption surface area and porosity. Journal of the Electrochemical Society, 114(11), 279C-279C.

Gruzdev, N., Pinto, R., & Sela, S. (2012). Persistence of *Salmonella enterica* during dehydration and subsequent cold storage. Food Microbiology, 32(2), 415-422.

Güçlü-Üstündağ, Ö., & Temelli, F. (2000). Correlating the solubility behavior of fatty acids, mono-, di-, and triglycerides, and fatty acid esters in supercritical carbon dioxide. Industrial & Engineering Chemistry Research, 39(12), 4756-4766.

Guggenheim, E. A. (1966). Applications of Statistical Mechanics. Clarendon Press.

Haas, G. J., Prescott Jr, H. E., Dudley, E., Dik, R., Hintlian, C., & Keane, L. (1989). Inactivation of microorganisms by carbon dioxide under pressure. Journal of Food Safety, 9(4), 253-265.

Hailwood, A. J., & Horrobin, S. (1946). Absorption of water by polymers: analysis in terms of a simple model. Transactions of the Faraday Society, 42, B084-B092.

Hara A, Radin NS. 1978. Lipid extraction of tissues with a low-toxicity solvent. Analytical and Bioanalytical Chemistry. 90: 420-426.

Health Canada. (2018). Food processing aids. https://www.canada.ca/en/health-canada/services/food-nutrition/food-safety/food-additives/processing-aids.html, (accessed on August 2, 2019).

Henderson, S. M. (1952). A basic concept of equilibrium moisture. Agricultural Engineering, 33, 29-32.

Hiramatsu, R., Matsumoto, M., Sakae, K., & Miyazaki, Y. (2005). Ability of Shiga toxin-producing *Escherichia coli* and *Salmonella* spp. to survive in a desiccation model system and in dry foods. Applied Environmental Microbiology, 71(11), 6657-6663.

Hong, S. I., & Pyun, Y. R. (2001). Membrane damage and enzyme inactivation of *Lactobacillus plantarum* by high pressure CO_2 treatment. International Journal of Food Microbiology, 63(1-2), 19-28.

Hong, S. I., Park, W. S., & Pyun, Y. R. (1999). Non-thermal inactivation of *Lactobacillus plantarum* as influenced by pressure and temperature of pressurized carbon dioxide. International Journal of Food Science & Technology, 34(2), 125-130.

Hossain, M. D., Bala, B. K., Hossain, M. A., & Mondol, M. R. A. (2001). Sorption isotherms and heat of sorption of pineapple. Journal of Food Engineering, 48(2), 103-107.

Hubinger, M. D., Vivanco-Pezantes, D., Kurozawa, L. E., & Sobral, P. J. (2009). Desorption isotherms of osmotically dehydrated and smoked Atlantic bonito (*Sarda sarda*) fillets. Revista Brasileira de Engenharia Agrícola e Ambiental, 13(3), 305-311.

Hutkins, R. W., & Nannen, N. L. (1993). pH homeostasis in lactic acid bacteria. Journal of Dairy Science, 76(8), 2354-2365.

Igbeka, J. C., & Blaisdell, J. L. (1982). Moisture isotherms of a processed meat product—Bologna. International Journal of Food Science & Technology, 17(1), 37-46.

Iglesias, H. (2012). Handbook of food isotherms: Water sorption parameters for food and food components. Elsevier. Amsterdam, The Netherlands.

Iglesias, H. A., & Chirife, J. (1976a). Isosteric heats of water vapor sorption on dehydrated foods. I. Analysis of the differential heat curves. LWT Lebensmittel-Wissenschaft Technologie.

Iglesias, H. A., & Chirife, J. (1976b). Equilibrium moisture contents of air dried beef. Dependence on drying temperature. International Journal of Food Science & Technology, 11(6), 565-573.

Iglesias, H. A., & Chirife, J. (1976c). Prediction of the effect of temperature on water sorption isotherms of food material. Journal of Food Technology, 11, 109-116

Iglesias, H. A., & Chirife, J. (1978). Local isotherm concept and modes of moisture binding in food products. Journal of Agricultural and Food Chemistry, 24(1), 77-79.

Iglesias, H. A., & Chirife, J. (1984). Correlation of BET monolayer moisture content in foods with temperature. International Journal of Food Science & Technology, 19(4), 503-506.

Iglesias, H. A., Chirife, J., & Lombardi, J. L. (1975). Comparison of water vapour sorption by sugar beet root components. International Journal of Food Science & Technology, 10(4), 385-391.

Isenschmid, A., Marison, I. W., & Von Stockar, U. (1995). The influence of pressure and temperature of compressed CO_2 on the survival of yeast cells. Journal of Biotechnology, 39(3), 229-237.

IUPAC. (1985). Reporting physisorption data for gas/solid systems. Commission on Colloidal and Surface Chemistry of the International Union of Pure and Applied Chemistry. Pure and Applied Chemistry 57: 603-619

Jakobsen, M., & Bertelsen, G. (2002). The use of CO_2 in packaging of fresh red meats and its effect on chemical quality changes in the meat: A review. Journal of Muscle Foods, 13(2), 143-168.

Jones, R. P., & Greenfield, P. F. (1982). Effect of carbon dioxide on yeast growth and fermentation. Enzyme and Microbial Technology, 4(4), 210-223.

Kajimoto, O. (1999). Solvation in supercritical fluids: its effects on energy transfer and chemical reactions. Chemical Reviews, 99(2), 355-390.

Kamihira, M., Taniguchi, M., & Kobayashi, T. (1987). Sterilization of microorganisms with supercritical carbon dioxide. Agricultural and Biological Chemistry, 51(2), 407-412.

Kapsalis, J. G. (1981). Moisture sorption hysteresis. In: Water Activity: Influences on Food Quality, eds. L. B. Rockland and G. E. Stewart, p. 143. New York: Academic Press

Kaya,S. and Kahyaoglu, T. 2005. Thermodynamic properties and sorption equilibrium of pestil (grape leather). Journal of Food Engineering, 71: 200-207.

Kimber, M. A., Kaur, H., Wang, L., Danyluk, M. D., & Harris, L. J. (2012). Survival of Salmonella, *Escherichia coli* O157: H7, and *Listeria monocytogenes* on inoculated almonds and pistachios stored at − 19, 4, and 24 ˚C. Journal of Food Protection, 75(8), 1394-1403.

King, M. B., Mubarak, A., Kim, J. D., & Bott, T. R. (1992). The mutual solubilities of water with supercritical and liquid carbon dioxide. The Journal of Supercritical Fluids, 5(4), 296-302.

King, Nicola J., and Rosemary Whyte. (2006). "Does it look cooked? A review of factors that influence cooked meat color." Journal of Food Science 71.4: R31-R40.

Kumagai, H., Hata, C., & Nakamura, K. (1997). CO_2 sorption by microbial cells and sterilization by high-pressure CO_2. Bioscience, Biotechnology, and Biochemistry, 61(6), 931-935.

Labuza TP and Albunakar B (2007). Water Activity Prediction and Moisture Sorption Isotherm. Water activity in Foods: Fundamentals and application. Ames, IA: Blackwell Publishing and IFT Press.

Labuza, T. P. (1971). Properties of water as related to the keeping quality of foods. Washington, DC, USA, In International Congress of Food Science and Technology. Proceedings.

Labuza, T. P. (1974). Interpretation of sorption data in relation to the state of constituent water. In Water relation of food: Proceedings of an International Symposium held in Glasgow, UK.

Labuza, T. P. (1980). The effect of water activity on reaction kinetics of food deterioration. Food Technology, 34(4), 36-41.

Labuza, T. P., Mizrahi, S., & Karel, M. (1972). Mathematical models for optimization of flexible film packaging of foods for storage. Transactions of the ASAE, 15(150).

Labuza, T.P. (1984). Moisture Sorption: Practical Aspects of Isotherm Measurement and Use. St. Paul, MN: AACC International Publishing.

Lewicki, P. P. (2004). Water as the determinant of food engineering properties. A review. Journal of Food Engineering, 61(4), 483-495.

Lin, H. M., Yang, Z., & Chen, L. F. (1992). Inactivation of *Saccharomyces cerevisiae* by supercritical and subcritical carbon dioxide. Biotechnology Progress, 8(5), 458-461.

Lin, H-M., Yang, Z.Y., Chen, L-F., (1993). Inactivation of *Leuconostoc dextranicum* with carbon dioxide under pressure. The Chemical Engineering Journal, 52(1), B29-B34.

Linko, P., Pollari, T., Harju, M., & Heikonen, M. (1982). Water sorption properties and the effect of moisture on structure of dried milk products. Lebensmittel-Wissenschaft Technologie, 15: 26-30.

Liouta, T. S., Bechtel, P. J., & Steinberg, M. P. (1984). Desorption and adsorption isotherms of meat-salt mixtures. Journal of Agricultural and Food Chemistry, 32(6), 1382-1385.

Luck, W. A. P. (1981). Structure of water in aqueous systems. In Water Activity: Influences on Food Quality, L. B. Rockland and G. F. Stewart (Eds.), pp. 407-434. Academic, New York.

Marcos, B., & Mullen, A. M. (2014). High pressure induced changes in beef muscle proteome: Correlation with quality parameters. Meat Science, 97(1), 11-20.

Martins, M. G., Martins, D. E. G., & da Silva Pena, R. (2015). Drying kinetics and hygroscopic behavior of pirarucu (Arapaima gigas) fillet with different salt contents. LWT-Food Science and Technology, 62(1), 144-151.

McCarty, K. A. (2016). Antimicrobial interventions applied to beef sub-primals for the control of *Escherichia coli* and their impact on ground beef quality. MSc Thesis, University of Nebraska-Lincoln. USA.

Meurehg, T., & Arturo, C. (2006). Control of *Escherichia coli* O157: h7, generic *Escherichia coli*, and *Salmonella* spp. on beef trimmings prior to grinding using a controlled phase carbon dioxide system, Doctoral dissertation, Kansas State University. USA.

Møller, J. K., & Skibsted, L. H. (2006). Myoglobins: the link between discoloration and lipid oxidation in muscle and meat. Química Nova, 29(6), 1270-1278.

Nakamura, K., Enomoto, A., Fukushima, H., Nagai, K., & Hakoda, M. (1994). Disruption of microbial cells by the flash discharge of high-pressure carbon dioxide. Bioscience, Biotechnology, and Biochemistry, 58(7), 1297-1301.

Nieto, E. A. (2010). Special Topics in Food Science Applied Thermodynamics.

Oswin, C. R. (1946). The kinetics of package life. III. The isotherm. Journal of the Society of Chemical Industry, 65(12), 419-421.

Owen, B. B., & Brinkley, S. R. (1941). Calculation of the effect of pressure upon ionic equilibria in pure water and in salt solutions. Chemical Reviews, 29(3), 461-474.

Palipane, K. B., & Driscoll, R. H. (1993). Moisture sorption characteristics of in-shell macadamia nuts. Journal of Food Engineering, 18(1), 63-76.

R Core Team (2018). R: A language and environment for statistical computing. R Foundation for Statistical Computing, Vienna, Austria. URL https://www.R-project.org/.

Rahman, M. S., Seo, J. K., Choi, S. G., Gul, K., & Yang, H. S. (2018). Physicochemical characteristics and microbial safety of defatted bovine heart and its lipid extracted with supercritical CO_2 and solvent extraction. Food Science and Technology, 97, 355-361.

Rao, M. A., Rizvi, S. S., Datta, A. K., & Ahmed, J. (2014). Thermodynamic properties of foods in dehydration, Engineering properties of foods. CRC press, pp. 239-310

Rastogi, N. K., Raghavarao, K. S. M. S., Balasubramaniam, V. M., Niranjan, K., & Knorr, D. (2007). Opportunities and challenges in high pressure processing of foods. Critical Reviews in Food Science and Nutrition, 47(1), 69-112.

Rizvi, S. E., Rao, M. A. (1986). Engineering properties of foods. Thermodynamic properties of food in dehydration. Marcel Dekker Inc, New York, pp. 223-309

Rockland, L. B., (1969), Water activity and storage stability, Food Technology 23: 1241-1251.

Rodrigues, I., Trindade, M. A., Caramit, F. R., Candoğan, K., Pokhrel, P. R., & Barbosa-Canovas, G. V. (2016). Effect of high pressure processing on physicochemical and microbiological properties of marinated beef with reduced sodium content. Innovative Food Science & Emerging Technologies, 38, 328-333.

Schmidt, A., Beermann, K., Bach, E., & Schollmeyer, E. (2005). Disinfection of textile materials contaminated with *E. coli* in liquid carbon dioxide. Journal of Cleaner Production, 13(9), 881-885.

Schultze DM. (2019). Effect of High-Pressure Carbon Dioxide on Desiccated *Escherichia coli* and Salmonella, MSc Thesis, University of Alberta, Canada.

Schumann, M. S., Kennick, W. H., & Rock, D. F. (1982). Effect of hot boning and prerigor pressurization of beef on factors of economic importance. Journal of Food Science, 47(3), 864-866.

Shelly J. Schmidt & Joo Won Lee (2012) Comparison between water vapor sorption isotherms obtained using the new dynamic dewpoint isotherm method and those obtained using the standard saturated salt slurry method, International Journal of Food Properties, 15:2, 236-248.

Sirisee, U., Hsieh, F., & Huff, H. E. (1998). Microbial safety of supercritical carbon dioxide processes 1. Journal of Food Processing and Preservation, 22(5), 387-403.

Spilimbergo, S. (2002). A study about the effect of dense CO_2 on microorganisms. PhD dissertation, University of Padova, Italy.

Spilimbergo, S., Bertucco, A., Basso, G., & Bertoloni, G. (2005). Determination of extracellular and intracellular pH of *Bacillus subtilis* suspension under CO_2 treatment. Biotechnology and Bioengineering, 92(4), 447-451.

Statistica, (2019) U.S. population: Consumption of meat snacks and beef jerky from 2011 to 2020. https://www.statista.com/statistics/282442/us-households-consumption-of-meat-snacks-and-beef-jerky-trend/ (accessed on August 2nd, 2019).

Sun, X. D., & Holley, R. A. (2010). High hydrostatic pressure effects on the texture of meat and meat products. Journal of Food Science, 75(1), R17-R23.

Suzuki, A., Kim, K., Homma, N., Ikeuchi, Y., and Saito, M. (1992) Acceleration of meat conditioning by high pressure treatment. In: High Pressure and Biotechnology. Balny, C., Hayashi, R., Heremans, K., and Masson, P. (eds) Institut Natl De LA Sante., Paris, France, pp. 219-227.

Szerman, N., Barrio, Y., Schroeder, B., Martinez, P., Sancho, A. M., Sanow, C., & Vaudagna, S. R. (2011). Effect of high hydrostatic pressure treatments on physicochemical properties, microbial quality and sensory attributes of beef carpaccio. Procedia Food Science, 1, 854-861.

Tabasinejad, F., Moore, R. G., Mehta, S. A., Van Fraassen, K. C., Barzin, Y., Rushing, J. A., & Newsham, K. E. (2011). Water solubility in supercritical methane, nitrogen, and carbon dioxide: measurement and modeling from 422 to 483 K and pressures from 3.6 to 134 MPa. Industrial & Engineering Chemistry Research, 50(7), 4029-4041.

Tassaing, T., Oparin, R., Danten, Y., & Besnard, M. (2005). Water–CO_2 interaction in supercritical CO_2 as studied by infrared spectroscopy and vibrational frequency shift calculations. The Journal of Supercritical Fluids, 33(1), 85-92.

Tucker, S. C. (1999). Solvent density inhomogeneities in supercritical fluids. Chemical Reviews, 99(2), 391-418.

Tsami, E., Maroulis, Z. B., Marinos-Kouris, D., & Saravacos, G. D. (1990). Heat of sorption of water in dried fruits. International Journal of Food Science and Technology, 25, 350-359.

Valley, G., & Rettger, L. F. (1927). The influence of carbon dioxide on bacteria. Journal of Bacteriology, 14(2), 101.

Vaudagna, S. R., Gonzalez, C. B., Guignon, B., Aparicio, C., Otero, L., & Sanz, P. D. (2012). The effects of high hydrostatic pressure at subzero temperature on the quality of ready-to-eat cured beef carpaccio. Meat Science, 92(4), 575-581.

Wang, Z., Zhou, Q., Guo, H., Yang, P., & Lu, W. (2018). Determination of water solubility in supercritical CO_2 from 313.15 to 473.15 K and from 10 to 50 MPa by in-situ quantitative Raman spectroscopy. Fluid Phase Equilibria, 476, 170-178.

Wei, C. I., Balaban, M. O., Fernando, S. Y., & Peplow, A. J. (1991). Bacterial effect of high pressure CO_2 treatment on foods spiked with Listeria or Salmonella. Journal of Food Protection, 54(3), 189-193.

Wheeler, T. L., Kalchayanand, N., & Bosilevac, J. M. (2014). Pre-and post-harvest interventions to reduce pathogen contamination in the US beef industry. Meat Science, 98(3), 372-382.

Yi, J., Zhang, L., Ding, G., Hu, X., Liao, X., & Zhang, Y. (2013). High hydrostatic pressure and thermal treatments for ready-to-eat wine-marinated shrimp: An evaluation of microbiological and physicochemical qualities. Innovative Food Science & Emerging Technologies, 20, 16–23.

Zhang, L., Sun, D. W., & Zhang, Z. (2017). Methods for measuring water activity (a_w) of foods and its applications to moisture sorption isotherm studies. Critical Reviews in Food Science and Nutrition, 57(5), 1052-1058.

Zhang, W., Xiao, S., Samaraweera, H., Lee, E. J., & Ahn, D. U. (2010). Improving functional value of meat products. Meat Science, 86(1), 15-31.

Zhao, L., Temelli, F., Curtis, J. M., & Chen, L. (2015). Preparation of liposomes using supercritical carbon dioxide technology: Effects of phospholipids and sterols. Food Research International, 77, 63-72.